

CDOpt: A Python Package for a Class of Riemannian Optimization

Nachuan Xiao · Xiaoyin Hu · Xin Liu ·
Kim-Chuan Toh

Received: date / Accepted: date

Abstract

Optimization over an embedded submanifold defined by equality constraints $c(x) = 0$ has attracted much interest over the past few decades due to its wide applications in various areas, including computer vision, signal processing, numerical linear algebra, and deep learning. For solving such problems, many related optimization packages have been developed based on Riemannian optimization approaches, which rely on some basic geometrical materials of Riemannian manifolds, including Riemannian gradients, retractions, vector transports, etc. These geometrical materials can be challenging to determine in general. In fact, existing packages only accommodate a few well-known manifolds whose geometrical materials are more easily accessible. For other manifolds that are not contained in these packages, the users have to develop the geometric materials by themselves. In addition, it is not always tractable to adapt the advanced features from various state-of-the-art unconstrained optimization solvers to Riemannian optimization approaches.

Here we introduce a user-friendly Python package, CDOpt (available at <https://cdopt.github.io/> under BSD 3-clause license), for solving a class of Riemannian optimization problems. CDOpt is designed to complement existing Riemannian optimization packages by transforming Riemannian optimization problems into their un-

Nachuan Xiao
The Institute of Operations Research and Analytics, National University of Singapore, Singapore.
E-mail: xnc@lsec.cc.ac.cn

Xiaoyin Hu
School of Computer and Computing Science, Hangzhou City University, Hangzhou, China.
Academy of Edge Intelligence, Hangzhou City University, Hangzhou(Gongshu), China.
E-mail: hxy@amss.ac.cn

Xin Liu
State Key Laboratory of Scientific and Engineering Computing, Academy of Mathematics and Systems Science, Chinese Academy of Sciences, and University of Chinese Academy of Sciences, China.
E-mail: liuxin@lsec.cc.ac.cn

Kim-Chuan Toh
Department of Mathematics, and Institute of Operations Research and Analytics, National University of Singapore, Singapore.
E-mail: mattohkc@nus.edu.sg

constrained counterparts through the constraint dissolving approach. We prove that when the penalty parameter in the constraint dissolving approach is sufficiently large, Riemannian optimization problems and their unconstrained counterparts are equivalent. Therefore, solving Riemannian optimization problems through CDOpt can directly benefit from various existing solvers and the rich expertise gained over the past few decades for unconstrained optimization. Moreover, all the computations in CDOpt related to any manifold in question are conducted through its constraints expression, hence users can easily define new manifolds in CDOpt without any background on differential geometry. Furthermore, CDOpt extends the neural layers from PyTorch and Flax, thus allowing users to train manifold constrained neural networks directly by the solvers for unconstrained optimization. Extensive numerical experiments demonstrate that CDOpt is highly efficient and robust in solving various classes of Riemannian optimization problems.

Keywords Riemannian optimization · Penalty function · Unconstrained optimization · Constraint dissolving

Mathematics Subject Classification (2020) 90C30 · 65K05

1 Introduction

1.1 Problem formulation

In this paper, we consider the following constrained optimization problem

$$\begin{aligned} \min_{x \in \mathbb{R}^n} \quad & f(x) \\ \text{s.t.} \quad & \mathcal{M} := \{x \in \mathbb{R}^n : c(x) = 0\}, \end{aligned} \tag{OCP}$$

where the objective function $f : \mathbb{R}^n \rightarrow \mathbb{R}$ and constraint mapping $c : \mathbb{R}^n \rightarrow \mathbb{R}^p$ of OCP satisfy the following assumptions:

Assumption 1 Blanket assumptions

1. f is locally Lipschitz continuous in \mathbb{R}^n ;
2. The transposed Jacobian of c , denoted as $J_c(x) \in \mathbb{R}^{n \times p}$, is locally Lipschitz continuous in \mathbb{R}^n ;
3. The relaxed constant rank constraint qualification (RCRCQ) [46] holds for any $x \in \mathcal{M}$, i.e. there exists a constant $p' \leq p$ and a neighborhood \mathcal{X} of \mathcal{M} such that the rank of $J_c(x)$ equals to p' for any $x \in \mathcal{X}$.

Since c is smooth in \mathbb{R}^n , the feasible region \mathcal{M} is a closed submanifold embedded in \mathbb{R}^n [4, 11]. In fact, OCP satisfying Assumption 1 covers a great number of practically interesting Riemannian optimization problems [28, 64] arising over the past few decades. These Riemannian optimization problems can be categorized into two different categories. One is the so-called *standard Riemannian optimization problem*, where the function value and derivatives of the objective function are explicitly formulated and affordable to evaluate, hence can be directly provided to optimization packages. These problems include the Kohn-Sham total energy minimization [6], dictionary learning [69], dual principal component pursuit [58, 29], symplectic eigenvalue problems [54],

etc. Interested readers may refer to the books [4, 11] and a recent survey paper [28] for more details of these problems.

Another category is referred as *training neural networks with manifold constraints* throughout this paper. Training deep neural networks (DNNs) is usually thought to be challenging both theoretically and practically, where the gradient vanishing and exploding problem is one of the most important reasons [23]. To address this issue, several recent works focus on training DNNs while imposing manifold constraints to the weights of their neural layers, especially on restricting the weights over the Stiefel manifold [5, 8, 33, 40]. As orthogonality can be used to impose energy preservation properties on these DNNs [71], some existing works demonstrate that the orthogonal constraints can stabilize the distribution of activations among neural layers within DNNs and make their optimization more efficient. Moreover, many existing works [8, 33, 61] observe encouraging improvements in the accuracy and robustness of the DNNs with orthogonally constrained weights.

In training neural networks with manifold constraints, the neural network is built by the composition of neural layers, while the objective function is formulated as the expectation of the losses over samples. Therefore, the function value and differentials of the objective function are usually unaffordable to be evaluated exactly, and most of the *optimizers* (i.e., solvers for training neural networks) are developed based on stochastic optimization algorithms to reduce the computational costs. Moreover, existing deep-learning frameworks (e.g. PyTorch [50], JAX [13], TensorFlow [1]) provide various advanced features, including GPU/TPU acceleration, automatic differentiation (AD), just-in-time compilation, to further accelerate the training. As a result, training neural networks with manifold constraints requires specialized optimization solvers (i.e., optimizers) to utilize the advanced features of these frameworks, which leads to great differences between their optimizers and the solvers for standard Riemannian optimization problems.

1.2 Existing approaches and optimization packages

Due to the diffeomorphisms between an Euclidean space and a Riemannian manifold, various *unconstrained optimization approaches* (i.e., approaches for solving unconstrained nonconvex optimization) can be transferred to their corresponding *Riemannian optimization approaches* (i.e., the approaches for Riemannian optimization). In particular, [4] provides several well-recognized frameworks based on geometrical materials from differential geometry, including geodesics, parallel transports, and Riemannian differentials.

The geodesics generalize the concept of straight lines to Riemannian manifolds, but are expensive to compute in most cases. To this end, [4] provides the concept of retractions as relaxations to geodesics, which makes them more affordable to compute. Besides, parallel transports are mappings that move tangent vectors along given curves over a Riemannian manifold “parallelly”. Computing parallel transports is essential in computing the linear combina-

tions of two vectors from different tangent spaces. In particular, it is necessary for those approaches that utilize information in past iterations (e.g., quasi-Newton methods, nonlinear conjugate gradient methods, momentum SGD, ADAM). For various Riemannian manifolds, computing the parallel transports amounts to solving differential equations, which is generally unaffordable in practice [4]. Therefore, the concept of vector transports is proposed as approximations to parallel transports to alleviate the computational cost in Riemannian optimization approaches. Although retractions and vector transports can make the computation more affordable by approximation, how to develop efficient formulations of retractions and vector transports for new manifold constraints remain challenging.

Almost all the existing Riemannian optimization packages are developed based on the framework proposed by [4]. These packages are either developed for standard Riemannian optimization problems (e.g., `Manopt` [12], `PyManopt` [57], `ROPTLIB` [34]), or specialized for training neural networks with manifold constraints (e.g., `Geoopt` [37], `McTorch` [45], `Rieoptax` [59]). In these packages, the manifold is described by the constraints, together with the geometrical materials from differential geometry, including retractions and their inverses, vector transports, etc. Some packages, including `Geomstats` [47], even require the exact formulation of exponential mappings and logarithm mappings. Unfortunately, the task of computing these geometrical materials is usually non-trivial. Although these existing Riemannian optimization packages provide several predefined manifolds based on various excellent works on determining the geometrical materials for some important manifolds [16, 48, 9, 21], it is still non-trivial to add new manifold constraints for users and developers, especially when they are nonexperts in differential geometry.

As manifold constraints are characterized by geometrical materials, Riemannian optimization solvers are developed from unconstrained optimization ones by incorporating these geometrical materials. To extend a large collection of unconstrained optimization solvers to its Riemannian versions, the following three steps are indispensable: (i) replace Euclidean differentials by Riemannian differentials; (ii) invoke retractions to keep the feasibility of the iterates; (iii) employ vector transports to move vectors among the tangent spaces of the manifolds. Therefore, building up new Riemannian optimization algorithms by borrowing the advanced features of state-of-the-art unconstrained optimization algorithms is challenging in general. Existing Riemannian optimization packages only provide limited Riemannian optimization algorithms. For example, compared with over 30 efficient optimizers from `PyTorch` and `PyTorch-optimizer` packages for unconstrained optimization, `Geoopt` only provides Riemannian Adam and Riemannian SGD, and `McTorch` is only integrated with Riemannian AdaDelta and Riemannian SGD.

Additionally, the package `GeoTorch` [40] is developed based on the trivialization approach for training neural networks with manifold constraints by `PyTorch`. In `GeoTorch`, the manifold is characterized by a smooth surjective mapping (trivialization mapping) $\psi : \mathbb{R}^N \rightarrow \mathcal{M}$ for some constant N . Then `GeoTorch` transforms OCP into the following unconstrained optimization prob-

lem,

$$\min_{u \in \mathbb{R}^N} f(\psi(u)).$$

However, determining the trivialization mapping ψ is usually as challenging as determining the geometrical materials of \mathcal{M} . Until now, the formulations of ψ are only determined for spheres and Stiefel manifolds.

On the other hand, although `GeoTorch` enables the direct implementation of unconstrained optimization solvers to OCP for spheres and Stiefel manifolds, the expression of trivialization mappings in `GeoTorch` are usually too complicated to be computed efficiently. As mentioned in [61, 63, 30, 2], computing the mapping ψ provided in `GeoTorch` is usually costly, and could become the major computational bottleneck for the optimizers. For example, when \mathcal{M} is chosen as the Stiefel manifold $\mathcal{S}_{m,s}$ embedded in $\mathbb{R}^{m \times s}$, ψ is chosen as the Cayley transform or matrix exponential of an $n \times n$ skew-symmetric matrix in `GeoTorch`. Then computing ψ and its differentials are extremely expensive, leading to its inferior performance when compared with other optimization approaches [61, 2, 30].

Apart from the trivialization approach, [2] introduces the landing method for minimizing continuously differentiable functions over the Stiefel manifold. Then following the framework of the landing method, [22] incorporates the canonical metric to the landing method [22], and [3] extends the landing method to solve stochastic optimization over the Stiefel manifold. Despite these advancements, these variants of the landing method are primarily developed based on the vanilla (stochastic) gradient descent method and do not integrate widely-used acceleration techniques (e.g., heavy-ball momentum, Nesterov momentum, adaptive stepsizes). Furthermore, the existing approaches derived from the landing method are mainly restricted to problems on the Stiefel manifold. The challenge of extending the landing method to address the broader class of problems represented by (OCP) remains an open question.

Furthermore, by regarding (OCP) as a constrained optimization problem, some existing penalty function approaches can be applied to solve (OCP). The nonsmooth penalty function approach [49] is a simple and fundamental approach for constrained optimization, where the penalty function can be expressed as,

$$\psi_{NS}(x) := f(x) + \beta \|c(x)\|.$$

However, the penalty function ψ_{NS} is nonsmooth even if f and c are continuously differentiable. Therefore, the minimization of ψ_{NS} is challenging in practice, as a wide range of efficient methods for smooth unconstrained optimization (e.g., quasi-Newton method, conjugate gradient method [19], trust-region method [51]) require the differentiability of the objective functions.

On the other hand, several existing works [17, 25] have developed exact penalty function approaches based on the Fletcher's penalty function [20] defined by

$$\psi_{FL}(x) := f(x) - \langle J_c(x)^\dagger \nabla f(x), c(x) \rangle + \beta \|c(x)\|^2.$$

Here $J_c(x)^\dagger$ is the pseudo-inverse of $J_c(x)$. However, the evaluation of $\psi_{FL}(x)$ requires the computation of $\nabla f(x)$, and computing the differentials of ψ_{FL} requires the computation of higher-order differentials of the objective function f . As a result, existing approaches based on Fletcher's penalty function, such as inexact steepest descent methods [17], inexact Newton methods [56, 55, 68], and inexact quasi-Newton methods [17], are usually combined with certain approximation strategies to waive the computation of higher-order derivatives. Hence, various existing unconstrained optimization approaches are not compatible with the Fletcher's penalty function framework.

Given the challenges in developing efficient Riemannian optimization approaches based on existing Riemannian optimization packages, we are driven to ask the following question:

Can we develop an optimization package that enables direct implementations of unconstrained optimization solvers for a Riemannian optimization problem, without the need to compute any geometrical materials of the corresponding manifold?

1.3 Developing optimization packages from the constraint dissolving approach

To directly apply unconstrained optimization approaches for solving Riemannian optimization problems, [64] proposed the *constraint dissolving* approach for OCP, under the assumption that linear independence constraint qualification (LICQ) holds at any feasible point of \mathcal{M} . The constraint dissolving approach transforms OCP into the unconstrained minimization of the following constraint dissolving function (CDF),

$$h(x) := f(\mathcal{A}(x)) + \frac{\beta}{2} \|c(x)\|^2. \quad (\text{CDF})$$

Here $\mathcal{A} : \mathbb{R}^n \rightarrow \mathbb{R}^n$ is called the constraint dissolving mapping, which should satisfy the following assumptions.

Assumption 2 Blanket assumptions on \mathcal{A}

- \mathcal{A} is locally Lipschitz smooth in \mathbb{R}^n ;
- $\mathcal{A}(x) = x$ holds for any $x \in \mathcal{M}$;
- The Jacobian of $c(\mathcal{A}(x))$ equals to 0 for any $x \in \mathcal{M}$. That is, $J_{\mathcal{A}}(x)J_c(x) = 0$ holds for any $x \in \mathcal{M}$, where $J_{\mathcal{A}}(x) \in \mathbb{R}^{n \times n}$ denotes the transposed Jacobian of \mathcal{A} at x .

The details on how to construct suitable constraint dissolving mappings \mathcal{A} for \mathcal{M} are presented in Section 4.1.

When f is assumed to be locally Lipschitz smooth, [64] proves that OCP and CDF have the same first-order stationary points, second-order stationary points, local minimizers, and Lojasiewicz exponents in a neighborhood of \mathcal{M} . More importantly, [64] shows that constructing CDF is completely independent of any geometrical material of \mathcal{M} . Therefore, we can develop various

constraint dissolving approaches to solve optimization problems over a broad class of manifolds embedded in \mathbb{R}^n , without any prior knowledge of their geometrical properties. Note that [64] analyze the relationships between OCP and CDF when LICQ holds everywhere on \mathcal{M} , which is a more stringent assumption than Assumption 1. Interested readers could further refer to [63, 65, 66] for developing constraint dissolving approaches and efficient algorithms for smooth optimization with orthogonality constraints.

For nonsmooth scenarios, [30] extends the constraint dissolving approaches for nonsmooth optimization over the Stiefel manifold, which enables the direct implementation of various existing unconstrained optimizers from PyTorch for training DNNs with orthogonally constrained weights. In another line of work, [31] shows that the feasible region of any nonconvex-strongly-convex bilevel optimization problem is a Riemannian manifold, and proposes a novel constraint dissolving approach for these bilevel optimization problems. Moreover, [31] develops a general framework for designing subgradient methods and proves their convergence properties for bilevel optimization problems.

However, these existing approaches either focus on specialized manifolds (e.g., Stiefel manifold), or require the global LICQ condition for the constraints $c(x)$. The development of constraint dissolving functions for (OCP) under more relaxed constraint qualifications has not been adequately addressed in the existing literature. More importantly, there is currently no software that is developed based on the constraint dissolving approach for solving Riemannian optimization problems. On the other hand, the penalty parameter β plays an important role in the exactness of the constraint dissolving function $h(x)$. Although [64] suggests a threshold value for β to guarantee the equivalence between OCP and CDF in a neighborhood of the manifold \mathcal{M} , such a threshold may be difficult to estimate. How to practically choose the penalty parameter β for CDF remains unexplored. In this paper, we will propose an easy-to-implement scheme for estimating the threshold value for the penalty parameter β .

1.4 Contributions

In this paper, we present a Python package called CDOpt, which is developed based on the constraint dissolving approaches for both standard Riemannian optimization problems and training neural networks with manifold constraints. Different from existing Riemannian optimization packages, CDOpt simultaneously achieves the following goals,

- **Dissolved constraints:** Developed based on the constraint dissolving approaches, CDOpt first transforms Riemannian optimization problems into unconstrained optimization problems. Therefore, we can utilize various highly efficient solvers for unconstrained optimization, and directly apply them to solve Riemannian optimization problems. Benefiting from the rich expertise gained over the past decades for unconstrained optimization, CDOpt is very efficient and naturally avoids the needs and difficulties

in extending the unconstrained optimization solvers to their Riemannian versions.

- **High compatibility:** CDOpt has high compatibility with various existing numerical backends, including NumPy [26], SciPy [60], Autograd [43], PyTorch [50], JAX [13] and Flax [27]. Users can directly apply the advanced features of these packages to accelerate the optimization, including automatic differentiation, GPU/TPU supports, just-in-time (JIT) compilation, etc.
- **Customized manifolds:** CDOpt dissolves manifold constraints without involving any geometrical material of the manifold in question. Therefore, users can directly define various Riemannian manifolds in CDOpt through their constraint expressions $c(x)$.
- **Plug-in neural layers:** CDOpt provides various plug-in neural layers for PyTorch and Flax packages. With minor changes to the standard PyTorch / Flax codes, users can easily build and train neural networks with various manifold constraints based on PyTorch and JAX.

These features make CDOpt an easy-to-use package complementing the existing Riemannian optimization packages, in the sense that CDOpt provides an alternative approach for Riemannian optimization by direct implementation of unconstrained solvers. Furthermore, we also present improved theoretical analysis on the relationships between CDF and OCP,

- **Relaxed constraint qualification:** We establish the equivalence between OCP and CDF under the RCRCQ condition, in the sense that OCP and CDF admit the same first-order and second-order stationary points in a neighborhood of \mathcal{M} . The involvement of the RCRCQ condition is weaker than the LICQ condition assumed in existing works [63, 64, 30, 31]. Therefore, the constraint dissolving approaches can be applied to the optimization problems over a broader class of embedded Riemannian submanifolds, including the Stiefel manifold with range constraints (i.e., the manifold studied in [35]).
- **Easy-to-implement scheme for tuning the penalty parameter:** We introduce a novel scheme for estimating the penalty parameter β for CDF to satisfy the exactness property in a neighborhood of \mathcal{M} . Compared with the threshold values presented in [64], which necessitate the determination of Lipschitz constants for f , \mathcal{A} and c , our proposed scheme only involves the computation of f , \mathcal{A} , c and their derivatives. In the CDOpt package, we employ the Monte Carlo sampling method to estimate the threshold value for the penalty parameter β based on our proposed scheme. As a result, CDOpt supports the automatic selection of β , hence overcoming the difficulties associated with choosing appropriate penalty parameters in existing constraint dissolving approaches.

1.5 Organizations

The rest of this paper is organized as follows. Section 2 presents some basic notations, definitions, and constants that are necessary for the theoretical analysis in later parts. We establish the theoretical properties of CDF and propose a practical scheme for choosing the penalty parameter in Section 3. Section 4 illustrates the structure of CDOpt and describes its main modules. In Section 5, we present a brief comparison between CDOpt and other existing Python Riemannian optimization packages. Section 4 exhibits several illustrative examples on applying CDOpt to solve standard Riemannian optimization problems and train neural networks with manifold constraints. Some examples on how to use CDOpt to solve Riemannian optimization problems are presented in Section 6. In Section 7, we present preliminary numerical experiments to illustrate that CDOpt enables efficient and direct implementation of various existing unconstrained solvers to solve OCP. We draw a brief conclusion in the last section.

2 Notations, definitions, and constants

2.1 Notations

Let $\text{range}(A)$ be the subspace spanned by the column vectors of matrix A , and $\|\cdot\|$ represents the ℓ_2 -norm of a vector or an operator. The notations $\text{diag}(A)$ and $\text{Diag}(x)$ stand for the vector formed by the diagonal entries of a matrix A , and the diagonal matrix with the entries of $x \in \mathbb{R}^n$ as its diagonal, respectively. We denote the smallest and largest eigenvalues of A by $\lambda_{\min}(A)$ and $\lambda_{\max}(A)$, respectively. Besides, $\sigma_s(A)$ refers to the s -th largest singular value of A while $\sigma_{\min}(A)$ refers to the smallest singular value of matrix A . Furthermore, for any matrix $A \in \mathbb{R}^{n \times p}$, the pseudo-inverse of A is denoted by $A^\dagger \in \mathbb{R}^{p \times n}$, which satisfies $AA^\dagger A = A$, $A^\dagger AA^\dagger = A^\dagger$, and both $A^\dagger A$ and AA^\dagger are symmetric [24].

In this paper, the Riemannian metric for \mathcal{M} is chosen as the Euclidean metric in \mathbb{R}^n . For any $x \in \mathcal{M}$, we denote the Riemannian gradient and Riemannian Hessian of f at x as $\text{grad } f(x)$ and $\text{hess } f(x)$, respectively.

For any $x \in \mathbb{R}^n$, we define the projection from $x \in \mathbb{R}^n$ to \mathcal{M} as

$$\text{proj}(x, \mathcal{M}) := \arg \min_{y \in \mathcal{M}} \|x - y\|.$$

It is worth mentioning that the optimality condition of the above problem leads to the fact that $x - w \in \text{range}(J_c(w))$ for any $w \in \text{proj}(x, \mathcal{M})$. Furthermore, $\text{dist}(x, \mathcal{M})$ refers to the distance between x and \mathcal{M} , i.e.

$$\text{dist}(x, \mathcal{M}) := \inf_{y \in \mathcal{M}} \|x - y\|.$$

We denote the transposed Jacobian of the mapping \mathcal{A} by $J_{\mathcal{A}}(x) \in \mathbb{R}^{n \times n}$. Let c_i and \mathcal{A}_i be the i -th coordinate of the mapping c and \mathcal{A} respectively, then

J_c and $J_{\mathcal{A}}$ can be expressed as

$$J_c(x) := \begin{bmatrix} \frac{\partial c_1(x)}{\partial x_1} & \dots & \frac{\partial c_p(x)}{\partial x_1} \\ \vdots & \ddots & \vdots \\ \frac{\partial c_1(x)}{\partial x_n} & \dots & \frac{\partial c_p(x)}{\partial x_n} \end{bmatrix} \in \mathbb{R}^{n \times p}, \quad \text{and } J_{\mathcal{A}}(x) := \begin{bmatrix} \frac{\partial \mathcal{A}_1(x)}{\partial x_1} & \dots & \frac{\partial \mathcal{A}_n(x)}{\partial x_1} \\ \vdots & \ddots & \vdots \\ \frac{\partial \mathcal{A}_1(x)}{\partial x_n} & \dots & \frac{\partial \mathcal{A}_n(x)}{\partial x_n} \end{bmatrix} \in \mathbb{R}^{n \times n}.$$

Besides, $\mathcal{D}_{J_{\mathcal{A}}}(x) : d \mapsto \mathcal{D}_{J_{\mathcal{A}}}(x)[d]$ denotes the second-order derivative of the mapping \mathcal{A} , which can be regarded as a linear mapping from \mathbb{R}^n to $\mathbb{R}^{n \times n}$ that satisfies $\mathcal{D}_{J_{\mathcal{A}}}(x)[d] = \lim_{t \rightarrow 0} \frac{1}{t} (J_{\mathcal{A}}(x + td) - J_{\mathcal{A}}(x))$. Similarly, $\mathcal{D}_{J_c}(x)$ refers to the second-order derivative of the mapping c that satisfies $\mathcal{D}_{J_c}(x)[d] = \lim_{t \rightarrow 0} \frac{1}{t} (J_c(x + td) - J_c(x)) \in \mathbb{R}^{n \times p}$. Additionally, we set

$$\mathcal{A}^k(x) := \underbrace{\mathcal{A}(\mathcal{A}(\dots \mathcal{A}(x) \dots))}_{k \text{ times}},$$

for $k \geq 1$, and define $\mathcal{A}^0(x) := x$, $\mathcal{A}^\infty(x) := \lim_{k \rightarrow +\infty} \mathcal{A}^k(x)$. Furthermore, we denote $g(x) := f(\mathcal{A}(x))$ and use $\nabla f(\mathcal{A}(x))$ to denote $\nabla f(z)|_{z=\mathcal{A}(x)}$ in the rest of this paper.

2.2 Definitions

We first state the first-order optimality condition of OCP as follows.

Definition 1 ([49]) *Given $x \in \mathbb{R}^n$, we say x is a first-order stationary point of OCP if there exists $\tilde{\lambda} \in \mathbb{R}^p$ that satisfies*

$$\begin{cases} \nabla f(x) - \sum_{i=1}^p \tilde{\lambda}_i \nabla c_i(x) = 0, \\ c(x) = 0. \end{cases} \quad (1)$$

For any given $x \in \mathcal{M}$, we define $\lambda(x)$ as

$$\lambda(x) := J_c(x)^\dagger \nabla f(x) \in \arg \min_{\lambda \in \mathbb{R}^p} \|\nabla f(x) - J_c(x)\lambda\|.$$

Then it can be easily verified that

$$\nabla f(x) = J_c(x)\lambda(x), \quad (2)$$

whenever x is a first-order stationary point of OCP.

As the Riemannian metric on \mathcal{M} is fixed as the Euclidean metric in \mathbb{R}^n , the following propositions present the closed-form expressions for the tangent space, normal space, Riemannian gradient $grad f(x)$ and Riemannian Hessian $hess f(x)$ for any $x \in \mathcal{M}$. The proofs of these propositions directly follow [4, 11], and hence are omitted for simplicity.

Proposition 1 *Given $x \in \mathcal{M}$, the tangent space of \mathcal{M} at x can be expressed as $\mathcal{T}_x = \{d \in \mathbb{R}^n : d^\top J_c(x) = 0\}$, while the normal space of \mathcal{M} at x can be expressed as $\mathcal{N}_x = \text{Range}(J_c(x))$.*

Definition 2 Given $x \in \mathbb{R}^n$, we say x is a second-order stationary point of OCP if x is a first-order stationary point of OCP and for any $d \in \mathcal{T}_x$, it holds that

$$d^\top \left(\nabla^2 f(x) - \sum_{i=1}^p \lambda_i(x) \nabla^2 c_i(x) \right) d \geq 0. \quad (3)$$

Proposition 2 The Riemannian gradient of f at x can be expressed as

$$\text{grad } f(x) = \nabla f(x) - J_c(x)\lambda(x). \quad (4)$$

Moreover, $\text{hess } f(x)$ can be expressed as the following self-adjoint linear transform $\text{hess } f(x) : \mathcal{T}_x \rightarrow \mathcal{T}_x$ such that

$$d^\top \text{hess } f(x) d = d^\top \left(\nabla^2 f(x) - \sum_{i=1}^p \lambda_i(x) \nabla^2 c_i(x) \right) d, \quad \text{for any } d \in \mathcal{T}_x.$$

Given $x \in \mathcal{M}$, the smallest eigenvalue of $\text{hess } f(x)$ is defined as

$$\lambda_{\min}(\text{hess } f(x)) := \min_{d \in \mathcal{T}_x, \|d\|=1} d^\top \text{hess } f(x) d.$$

Let U_x be a matrix whose columns form an orthonormal basis of \mathcal{T}_x , we define the projected Hessian of OCP at x as

$$\mathcal{H}(x) := U_x^\top \left(\nabla^2 f(x) - \sum_{i=1}^p \lambda_i(x) \nabla^2 c_i(x) \right) U_x, \quad (5)$$

The following proposition characterizes the relationship between $\mathcal{H}(x)$ and $\text{hess } f(x)$.

Proposition 3 Given any $x \in \mathcal{M}$, suppose x is a first-order stationary point of OCP, then $\mathcal{H}(x)$ and $\text{hess } f(x)$ have the same eigenvalues. Moreover, we have that $\lambda_{\min}(\text{hess } f(x)) = \lambda_{\min}(\mathcal{H}(x))$ and x is a second-order stationary point of OCP if and only if $\mathcal{H}(x) \succeq 0$.

The proof of the above proposition directly follows from Proposition 2 and [4], and hence we omit it for simplicity.

Definition 3 Given $x \in \mathbb{R}^n$, we say x is a first-order stationary point of CDF if

$$\nabla h(x) = 0. \quad (6)$$

Moreover, when h is twice differentiable, we say $x \in \mathbb{R}^n$ is a second-order stationary point of h if x is a first-order stationary point of h and satisfies

$$\nabla^2 h(x) \succeq 0. \quad (7)$$

2.3 Constants

As illustrated in Assumption 1, the rank of $J_c(x)$ equals p' for any x in \mathcal{X} , which is a neighborhood of \mathcal{M} . Then for any given $x \in \mathcal{M}$, we define the positive scalar $\rho_x \leq 1$ as

$$\rho_x := \arg \max_{0 < \rho \leq 1, \mathcal{B}_{x,\rho} \subset \mathcal{X}} \rho \quad \text{s.t.} \quad \inf \{ \sigma_{p'}(J_c(y)) : y \in \mathcal{B}_{x,\rho} \} \geq \frac{1}{2} \sigma_{p'}(J_c(x)).$$

Based on the definition of ρ_x , we can define the set $\Theta_x := \{y \in \mathbb{R}^n : \|y - x\| \leq \rho_x\}$ and define several constants as follows:

- $\sigma_{x,c} := \sigma_{p'}(J_c(x))$;
- $M_{x,f} := \sup_{y \in \Theta_x} \|\nabla f(\mathcal{A}(y))\|$;
- $M_{x,c} := \sup_{y \in \Theta_x} \|J_c(y)\|$;
- $M_{x,A} := \sup_{y \in \Theta_x} \|J_{\mathcal{A}}(y)\|$;
- $L_{x,g} := \sup_{y,z \in \Theta_x, y \neq z} \frac{\|\nabla g(y) - \nabla g(z)\|}{\|y - z\|}$;
- $L_{x,c} := \sup_{y,z \in \Theta_x, y \neq z} \frac{\|J_c(y) - J_c(z)\|}{\|y - z\|}$;
- $L_{x,A} := \sup_{y,z \in \Theta_x, y \neq z} \frac{\|J_{\mathcal{A}}(y) - J_{\mathcal{A}}(z)\|}{\|y - z\|}$;
- $L_{x,b} := \sup_{y,z \in \Theta_x, y \neq z} \frac{\|J_{\mathcal{A}}(y)J_c(\mathcal{A}(y)) - J_{\mathcal{A}}(z)J_c(\mathcal{A}(z))\|}{\|y - z\|}$.

It should be noted that the constants mentioned above are primarily utilized for theoretical analysis to establish the relationships between OCP and CDF. In particular, the threshold value given in Definition 4 in Section 3 for β to ensure the equivalence between OCP and CDF, is free of the constants mentioned above. Consequently, it is not necessary to compute these aforementioned constants in the practical implementations of the CDOpt package.

Based on these constants, we further set

$$\varepsilon_x := \min \left\{ \frac{\rho_x}{2}, \frac{\sigma_{x,c}}{32L_{x,c}(M_{x,A} + 1)}, \frac{\sigma_{x,c}^2}{8(L_{x,b} + L_{x,c})M_{x,c}}, \frac{\sigma_{x,c}}{5(L_{x,b} + L_{x,A}M_{x,c})} \right\},$$

and define the following sets:

- $\Omega_x := \{y \in \mathbb{R}^n : \|y - x\| \leq \varepsilon_x\}$;
- $\bar{\Omega}_x := \left\{ y \in \mathbb{R}^n : \|y - x\| \leq \frac{\sigma_{x,c}\varepsilon_x}{4M_{x,c}(M_{x,A} + 1) + \sigma_{x,c}} \right\}$;
- $\bar{\Omega} := \bigcup_{x \in \mathcal{M}} \bar{\Omega}_x$;
- $\bar{\Omega} := \bigcup_{x \in \mathcal{M}} \bar{\Omega}_x$.

It is worth mentioning that Assumption 1 guarantees that $\sigma_{x,c} > 0$ for any given $x \in \mathcal{M}$, which implies that $\varepsilon_x > 0$. On the other hand, we can conclude that $\bar{\Omega}_x \subset \Omega_x \subset \Theta_x$ holds for any given $x \in \mathcal{M}$, and \mathcal{M} lies in the interior of $\bar{\Omega}$.

Finally, the following assumption is needed in analyzing the second-order stationarity of CDF.

Assumption 3 Assumption on second-order differentiability

- f, c and \mathcal{A} are twice differentiable in \mathbb{R}^n .

3 Theoretical Properties

In this section, we present the theoretical analysis on the relationships between the stationary point of OCP and those of CDF under the RCRCQ condition. We first establish some basic properties of the constraint dissolving mapping \mathcal{A} in Section 3.1. Based on these theoretical properties of \mathcal{A} , we propose a practical scheme on choosing the threshold value for penalty parameter β for CDF, and discuss how to compute the threshold value in practice. Finally, we prove that for any penalty β larger than the proposed threshold value, OCP and CDF have the same first-order and second-order stationary points in a neighborhood of \mathcal{M} .

3.1 Theoretical properties of \mathcal{A}

In this subsection, we aim to establish the same theoretical results as [64, Section 3.1] under Assumption 1, where we only assume that RCRCQ holds for every feasible point of OCP. We start by evaluating the relationships among $\|c(x)\|$, $\|c(\mathcal{A}(x))\|$ and $\text{dist}(x, \mathcal{M})$ in the following lemmas.

Lemma 1 *For any given $x \in \mathcal{M}$, the following inequalities hold for any $y \in \Omega_x$,*

$$\frac{1}{M_{x,c}} \|c(y)\| \leq \text{dist}(y, \mathcal{M}) \leq \frac{2}{\sigma_{x,c}} \|c(y)\|. \quad (8)$$

Proof Let $z \in \text{proj}(y, \mathcal{M})$, then from the definition of z we can conclude that $\|z - y\| \leq \|y - x\|$. Thus $\|z - x\| \leq \|z - y\| + \|y - x\| \leq 2\varepsilon_x \leq \rho_x$, and hence $z \in \Theta_x$. By the mean-value theorem, for any fixed $\nu \in \mathbb{R}^p$ there exists a point $\xi_\nu \in \mathbb{R}^n$ that is a convex combination of y and z such that $\nu^\top c(y) = (y - x)^\top J_c(\xi_\nu)\nu$. By the convexity of Θ_x , $\xi_\nu \in \Theta_x$ holds for any $\nu \in \mathbb{R}^p$. Therefore, we get

$$\begin{aligned} \|c(y)\| &= \sup_{\nu \in \mathbb{R}^p, \|\nu\|=1} \nu^\top c(y) = \sup_{\nu \in \mathbb{R}^p, \|\nu\|=1} (y - x)^\top J_c(\xi_\nu)\nu \\ &\leq \sup_{\xi_\nu \in \Theta_x} \|J_c(\xi_\nu)\| \|y - z\| \leq M_{x,c} \text{dist}(y, \mathcal{M}). \end{aligned}$$

Moreover, it follows from the definition of z that $y - z \in \text{range}(J_c(z))$. As a result, let $\tilde{\nu} = \frac{J_c(z)^\top (y-z)}{\|J_c(z)^\top (y-z)\|}$, we have

$$\begin{aligned} \|c(y)\| &= \sup_{\nu \in \mathbb{R}^p, \|\nu\|=1} (y - z)^\top J_c(\xi_\nu)\nu \geq (y - z)^\top J_c(\xi_{\tilde{\nu}})\tilde{\nu} \\ &= (y - z)^\top J_c(z)\tilde{\nu} + (y - z)^\top (J_c(z) - J_c(\xi_{\tilde{\nu}}))\tilde{\nu} \\ &= \|J_c(z)^\top (y - z)\| + (y - z)^\top (J_c(z) - J_c(\xi_{\tilde{\nu}}))\tilde{\nu} \\ &\geq \|J_c(z)^\top (y - z)\| - L_{x,c} \|y - z\|^2 \\ &\geq (\sigma_{x,c} - \varepsilon_x L_{x,c}) \text{dist}(y, \mathcal{M}) \geq \frac{\sigma_{x,c}}{2} \text{dist}(y, \mathcal{M}). \end{aligned}$$

Lemma 2 For any given $x \in \mathcal{M}$, it holds that

$$\|\mathcal{A}(y) - y\| \leq \frac{2(M_{x,A} + 1)}{\sigma_{x,c}} \|c(y)\|, \quad \text{for any } y \in \Omega_x. \quad (9)$$

Proof For any given $y \in \Omega_x$, we choose $z \in \text{proj}(y, \mathcal{M})$. Then we can conclude that $z \in \Theta_x$. Furthermore, from the Lipschitz continuity of \mathcal{A} and the fact that $\mathcal{A}(z) - z = 0$, it holds that

$$\begin{aligned} \|\mathcal{A}(y) - y\| &= \|(\mathcal{A}(y) - y) - (\mathcal{A}(z) - z)\| \leq (M_{x,A} + 1) \text{dist}(y, \mathcal{M}) \\ &\leq \frac{2(M_{x,A} + 1)}{\sigma_{x,c}} \|c(y)\|, \end{aligned} \quad (10)$$

where the last inequality follows from Lemma 1.

Lemma 3 For any given $x \in \mathcal{M}$, it holds that

$$\|c(\mathcal{A}(y))\| \leq \frac{4L_{x,b}}{\sigma_{x,c}^2} \|c(y)\|^2, \quad \text{for any } y \in \Omega_x. \quad (11)$$

Proof For any given $y \in \Omega_x$, we choose $z \in \text{proj}(y, \mathcal{M})$. It holds that $z \in \Theta_x$. By the mean-value theorem, for any $\nu \in \mathbb{R}^p$, there exists $t_\nu \in [0, 1]$ and $\xi_\nu = t_\nu y + (1 - t_\nu)z$ such that

$$\nu^\top c(\mathcal{A}(y)) = \nu^\top (J_{\mathcal{A}}(\xi_\nu) J_c(\mathcal{A}(\xi_\nu)))^\top (y - z). \quad (12)$$

The convexity of Θ_x ensures that $\xi_\nu \in \Theta_x$ holds for any $\nu \in \mathbb{R}^p$. Therefore, from the definition of $L_{x,b}$ and Ω_x , we get

$$\begin{aligned} \|c(\mathcal{A}(y))\| &= \sup_{\nu \in \mathbb{R}^p, \|\nu\|=1} \nu^\top c(\mathcal{A}(y)) \\ &= \sup_{\nu \in \mathbb{R}^p, \|\nu\|=1} \nu^\top (J_{\mathcal{A}}(\xi_\nu) J_c(\mathcal{A}(\xi_\nu)))^\top (y - z) \\ &\leq \sup_{\nu \in \mathbb{R}^p, \|\nu\|=1} \left\| (J_{\mathcal{A}}(\xi_\nu) J_c(\mathcal{A}(\xi_\nu)))^\top (y - z) \right\| \\ &\leq \sup_{\nu \in \mathbb{R}^p, \|\nu\|=1} \|J_{\mathcal{A}}(\xi_\nu) J_c(\mathcal{A}(\xi_\nu))\| \text{dist}(y, \mathcal{M}) \\ &\leq L_{x,b} \sup_{\nu \in \mathbb{R}^p, \|\nu\|=1} \|\xi_\nu - z\| \text{dist}(y, \mathcal{M}) \leq L_{x,b} \text{dist}(y, \mathcal{M})^2 \\ &\leq \frac{4L_{x,b}}{\sigma_{x,c}^2} \|c(y)\|^2, \end{aligned} \quad (13)$$

where the last inequality follows from Lemma 1.

For any given $x \in \mathcal{M}$ and $y \in \Omega_x$, Lemma 3 illustrates that the operator \mathcal{A} can reduce the feasibility violation of y quadratically when y is sufficiently close to \mathcal{M} . Moreover, the following lemma illustrates that although $J_c(x)$ may be singular for some $x \in \mathcal{M}$, $\|J_c(y)c(y)\|$ is still proportional to $\|c(y)\|$ for any $y \in \Omega_x$.

Lemma 4 For any given $x \in \mathcal{M}$ and any $y \in \Omega_x$, it holds that

$$\|J_c(y)c(y)\| \geq \frac{\sigma_{x,c}}{2} \|c(y)\|. \quad (14)$$

Proof For any given $y \in \Omega_x$, we choose $z \in \text{proj}(y, \mathcal{M})$. Therefore, for any $\nu \in \mathbb{R}^p$, there exists $t_\nu \in [0, 1]$ and $\xi_\nu = t_\nu y + (1 - t_\nu)z$ such that

$$\nu^\top c(y) = \nu^\top J_c(\xi_\nu)^\top (y - z) \geq \nu^\top J_c(y)^\top (y - z) - L_{x,c} \|y - z\|^2. \quad (15)$$

Then we can conclude that $\|c(y) - J_c(y)^\top (y - z)\| \leq L_{x,c} \|y - z\|^2$, which leads to

$$\begin{aligned} \|J_c(y)c(y)\| &\geq \|J_c(y)J_c(y)^\top (y - z)\| - L_{x,c}M_{x,c} \|y - z\|^2 \\ &\geq \sigma_{x,c} \|J_c(y)^\top (y - z)\| - L_{x,c}M_{x,c} \|y - z\|^2 \\ &\geq \sigma_{x,c} \|c(y)\| - (L_{x,c}M_{x,c} + \sigma_{x,c}L_{x,c}) \|y - z\|^2 \\ &\stackrel{(i)}{=} \sigma_{x,c} \|c(y)\| - (L_{x,c}M_{x,c} + \sigma_{x,c}L_{x,c}) (\text{dist}(y, \mathcal{M}))^2 \\ &\stackrel{(ii)}{\geq} \left(\sigma_{x,c} - \frac{2(L_{x,c}M_{x,c} + \sigma_{x,c}L_{x,c})}{\sigma_{x,c}} \text{dist}(y, \mathcal{M}) \right) \|c(y)\| \stackrel{(iii)}{\geq} \frac{\sigma_{x,c}}{2} \|c(y)\|, \end{aligned} \quad (16)$$

where (i) holds from the definition of z and (ii) directly follows from Lemma 1. Moreover, (iii) holds from the definitions for Ω_x and ε_x , which illustrate that

$$\begin{aligned} \text{dist}(y, \mathcal{M}) &\leq \|y - x\| \leq \varepsilon_x \\ &= \min \left\{ \frac{\rho_x}{2}, \frac{\sigma_{x,c}}{32L_{x,c}(M_{x,A} + 1)}, \frac{\sigma_{x,c}^2}{8(L_{x,b} + L_{x,c})M_{x,c}} \right\} \\ &\leq \left\{ \frac{\sigma_{x,c}^2}{32\sigma_{x,c}L_{x,c}}, \frac{\sigma_{x,c}^2}{8L_{x,c}M_{x,c}} \right\} \leq \frac{\sigma_{x,c}^2}{4L_{x,c}M_{x,c} + 16\sigma_{x,c}L_{x,c}} \\ &\leq \frac{\sigma_{x,c}^2}{4(L_{x,c}M_{x,c} + \sigma_{x,c}L_{x,c})}. \end{aligned}$$

This completes the proof.

In the rest of this subsection, we present the theoretical property of \mathcal{A}^∞ and $J_{\mathcal{A}}$ in Lemma 5 - Lemma 8, whose proofs directly follow the routines in [64, Section 3] and thus are omitted for simplicity.

Lemma 5 For any given $x \in \mathcal{M}$ and any $y \in \bar{\Omega}_x$, $\mathcal{A}^\infty(y)$ exists and $\mathcal{A}^\infty(y) \in \Omega_x \cap \mathcal{M}$. Moreover, it holds that

$$\|\mathcal{A}^\infty(y) - y\| \leq \frac{4(M_{x,A} + 1)}{\sigma_{x,c}} \|c(y)\|. \quad (17)$$

Lemma 6 For any given $x \in \mathcal{M}$, the inclusion $J_{\mathcal{A}}(x)^\top d \in \mathcal{T}_x$ holds for any $d \in \mathbb{R}^n$. Moreover, when $d \in \mathcal{T}_x$, it holds that $J_{\mathcal{A}}(x)^\top d = d$.

Lemma 7 For any given $x \in \mathcal{M}$, the equality $J_{\mathcal{A}}(x)d = 0$ holds if and only if $d \in \mathcal{N}_x$.

Lemma 8 For any given $x \in \mathcal{M}$, it holds that $J_{\mathcal{A}}(x)^2 = J_{\mathcal{A}}(x)$.

3.2 Selection of the penalty parameter

In this subsection, we discuss how to practically choose an appropriate penalty parameter for CDF. We first consider the threshold value for the penalty parameter β in CDF defined in the following definition.

Definition 4 For any given $x \in \mathcal{M}$, we set

$$\tilde{\beta}_x := \sup_{y \in \Omega_x} \left\{ \max \left\{ \frac{2(f(\mathcal{A}^2(y)) - f(\mathcal{A}(y)))}{\|c(y)\|^2 - \|c(\mathcal{A}(y))\|^2}, \frac{(\mathcal{A}(y) - y)^\top J_{\mathcal{A}}(y) \nabla f(\mathcal{A}(y))}{(y - \mathcal{A}(y))^\top J_c(y) c(y)}, 0 \right\} \right\}.$$

We first show that $\tilde{\beta}_x < +\infty$ for any $x \in \mathcal{M}$ in the following proposition.

Proposition 4 For any $x \in \mathcal{M}$, it holds that

$$\tilde{\beta}_x \leq \max \left\{ \frac{64M_{x,f}(M_{x,A} + 1)L_{x,b}}{3\sigma_{x,c}^3}, \frac{(24L_{x,A}M_{x,A} + 8L_{x,A})M_{x,f}}{\sigma_{x,c}^2} \right\}.$$

Proof Firstly, it directly follows from [64, Proposition 4.2] that

$$\sup_{y \in \Omega_x} \left\{ \frac{2(f(\mathcal{A}^2(y)) - f(\mathcal{A}(y)))}{\|c(y)\|^2 - \|c(\mathcal{A}(y))\|^2} \right\} \leq \frac{64M_{x,f}(M_{x,A} + 1)L_{x,b}}{3\sigma_{x,c}^3}.$$

Moreover, for any $x \in \mathcal{M}$ and any $y \in \Omega_x$, let $z \in \text{proj}(y, \mathcal{M})$, it holds from Lemma 1 that

$$\begin{aligned} |(y - z)^\top J_{\mathcal{A}}(y) J_c(y) c(y)| &\leq \|y - z\| \|c(y)\| \|J_{\mathcal{A}}(y) J_c(y)\| \\ &\leq L_{x,b} \|y - z\| \|c(y)\| \text{dist}(y, \mathcal{M}) = L_{x,b} \|y - z\|^2 \|c(y)\|. \end{aligned} \quad (18)$$

Then there exists $\xi = ty + (1 - t)z$ for some $t \in [0, 1]$ such that

$$\begin{aligned} (y - \mathcal{A}(y))^\top J_c(y) c(y) &= (y - z)^\top (I_n - J_{\mathcal{A}}(\xi)) J_c(y) c(y) \\ &\geq (y - z)^\top J_c(y) c(y) - |(y - z)^\top J_{\mathcal{A}}(y) J_c(y) c(y)| - L_{x,A} M_{x,c} \|y - z\|^2 \|c(y)\|. \end{aligned}$$

Now by the mean-value theorem, for some $\nu = sy + (1 - s)z$ with $s \in [0, 1]$, we have that $c(y)^\top c(y) = (c(y) - c(z))^\top c(y) = (y - z)^\top J_c(\nu) c(y) = (y - z)^\top J_c(y) c(y) + (y - z)^\top (J_c(\nu) - J_c(y)) c(y)$. Thus

$$\begin{aligned} &(y - \mathcal{A}(y))^\top J_c(y) c(y) \\ &\geq \|c(y)\|^2 - |(y - z)^\top (J_c(\nu) - J_c(y)) c(y)| \\ &\quad - |(y - z)^\top J_{\mathcal{A}}(y) J_c(y) c(y)| - L_{x,A} M_{x,c} \|y - z\|^2 \|c(y)\| \\ &\stackrel{(i)}{\geq} \frac{\sigma_{x,c}}{2} \|y - z\| \|c(y)\| - L_{x,c} \|y - z\|^2 \|c(y)\| \\ &\quad - L_{x,b} \|y - z\|^2 \|c(y)\| - L_{x,A} M_{x,c} \|y - z\|^2 \|c(y)\| \\ &\stackrel{(ii)}{\geq} \frac{15\sigma_{x,c}}{32} \|y - z\| \|c(y)\| - (L_{x,A} M_{x,c} + L_{x,b}) \|y - z\|^2 \|c(y)\| \\ &\stackrel{(iii)}{\geq} \frac{\sigma_{x,c}}{4} \|y - z\| \|c(y)\|. \end{aligned}$$

Here (i) uses (18), (ii) follows from the fact that $\|y - z\| \leq \varepsilon_x \leq \frac{\sigma_{x,c}}{32L_{x,c}}$, and (iii) holds from the fact that $(L_{x,A}M_{x,c} + L_{x,b})\|y - z\| \leq (L_{x,A}M_{x,c} + L_{x,b})\varepsilon_x \leq \frac{1}{5}$. Together with Lemma 1, we achieve that

$$(y - \mathcal{A}(y))^\top J_c(y)c(y) \geq \frac{\sigma_{x,c}}{4M_{x,c}} \|c(y)\|^2. \quad (19)$$

Moreover, from the mean-value theorem, it holds from the Lipschitz continuity of $J_{\mathcal{A}}(y)$ and Lemma 8 that

$$\begin{aligned} & |(y - z)^\top (I_n - J_{\mathcal{A}}(y))J_{\mathcal{A}}(y)\nabla f(\mathcal{A}(y))| \\ & \leq \|J_{\mathcal{A}}(y) - J_{\mathcal{A}}(y)\|^2 M_{x,f} \|y - z\| \\ & \leq L_{x,A}(2M_{x,A} + 1)\text{dist}(y, \mathcal{M})M_{x,f} \|y - z\| \\ & = L_{x,A}(2M_{x,A} + 1)M_{x,f} \|y - z\|^2. \end{aligned} \quad (20)$$

As a result, we have

$$\begin{aligned} & |(y - \mathcal{A}(y))^\top J_{\mathcal{A}}(y)\nabla f(\mathcal{A}(y))| \\ & \leq |(y - z)^\top (I_n - J_{\mathcal{A}}(y))J_{\mathcal{A}}(y)\nabla f(\mathcal{A}(y))| \\ & \quad + |(y - z)^\top (J_{\mathcal{A}}(\xi) - J_{\mathcal{A}}(y))J_{\mathcal{A}}(y)\nabla f(\mathcal{A}(y))| \\ & \leq L_{x,A}(2M_{x,A} + 1)M_{x,f} \|y - z\|^2 + L_{x,A}M_{x,A}M_{x,f} \|y - z\|^2 \\ & \leq \frac{(6L_{x,A}M_{x,A} + 2L_{x,A})M_{x,f}}{\sigma_{x,c}} \|c(y)\| \|y - z\|, \end{aligned}$$

where the first inequality is obtained by applying the mean-value theorem to $(y - \mathcal{A}(y))^\top J_{\mathcal{A}}(y)\nabla f(\mathcal{A}(y)) = ((y - \mathcal{A}(y)) - (z - \mathcal{A}(z)))^\top J_{\mathcal{A}}(y)\nabla f(\mathcal{A}(y)) = (y - z)^\top (I_n - J_{\mathcal{A}}(\xi))J_{\mathcal{A}}(y)\nabla f(\mathcal{A}(y))$ for some $\xi = ty + (1 - t)z$ such that $t \in [0, 1]$.

Therefore, for any $y \in \Omega_x$, we obtain

$$\begin{aligned} \left| \frac{(y - \mathcal{A}(y))^\top J_{\mathcal{A}}(y)\nabla f(\mathcal{A}(y))}{(y - \mathcal{A}(y))^\top J_c(y)c(y)} \right| & \leq \frac{\frac{(6L_{x,A}M_{x,A} + 2L_{x,A})M_{x,f}}{\sigma_{x,c}} \|c(y)\| \|y - z\|}{\frac{\sigma_{x,c}}{4} \|c(y)\| \|y - z\|} \\ & \leq \frac{(24L_{x,A}M_{x,A} + 8L_{x,A})M_{x,f}}{\sigma_{x,c}^2}. \end{aligned}$$

This completes the proof.

Remark 1 As illustrated in Proposition 4, $\tilde{\beta}_x$ is well-defined for any given $x \in \mathcal{M}$. To estimate the value of $\tilde{\beta}_x$ from f, \mathcal{A}, c and their derivatives, we can employ various approaches for estimating $\tilde{\beta}_x$, such as Monte Carlo sampling, Markov chain Monte Carlo (MCMC) sampling, etc. For example, when employing the Monte Carlo sampling method for choosing the penalty parameter for CDF, we can first choose a reference point $\tilde{x} \in \mathcal{M}$ and randomly sample

N_β points $\{x_1^{ref}, \dots, x_{N_\beta}^{ref}\} \in \mathcal{B}(\tilde{x}, \delta_\beta) := \{x \in \mathbb{R}^n : \|x - \tilde{x}\| \leq \delta_\beta\}$. Then we compute an estimated value for $\tilde{\beta}_x$, denoted as $\tilde{\beta}_x^*$, by the following scheme,

$$\tilde{\beta}_x^* = \theta_\beta \cdot \max_{1 \leq i \leq N_\beta} \left\{ \max \left\{ \frac{2(f(\mathcal{A}^2(x_i^{ref})) - f(\mathcal{A}(x_i^{ref})))}{\left| \|c(x_i^{ref})\|^2 - \|c(\mathcal{A}(x_i^{ref}))\|^2 \right| + \varepsilon_\beta}, \right. \right. \\ \left. \left. \frac{(\mathcal{A}(x_i^{ref}) - x_i^{ref})^\top J_{\mathcal{A}}(x_i^{ref}) \nabla f(\mathcal{A}(x_i^{ref}))}{\left| (x_i^{ref} - \mathcal{A}(x_i^{ref}))^\top J_c(x_i^{ref}) c(x_i^{ref}) \right| + \varepsilon_\beta}, 0 \right\} \right\}. \quad (21)$$

Here $\delta_\beta > 0$, $\varepsilon_\beta \geq 0$ and $\theta_\beta \geq 1$ are some prefixed hyper-parameters.

When Assumption 3 holds, it is easy to verify that the function

$$\phi_{\beta,x}(y) := \max \left\{ \frac{2(f(\mathcal{A}^2(y)) - f(\mathcal{A}(y)))}{\|c(y)\|^2 - \|c(\mathcal{A}(y))\|^2}, \frac{(\mathcal{A}(y) - y)^\top J_{\mathcal{A}}(y) \nabla f(\mathcal{A}(y))}{(y - \mathcal{A}(y))^\top J_c(y) c(y)}, 0 \right\} \quad (22)$$

is continuous over $\Omega_x \setminus x$ for any $x \in \mathcal{M}$. Therefore, with $\delta_\beta \geq \sup_{y \in \Omega_x} \|y - x\|$, $\theta_\beta \geq 1$, and $\varepsilon_\beta = 0$, our sampling technique guarantees that $\lim_{N_\beta \rightarrow +\infty} \tilde{\beta}_x^* \geq \tilde{\beta}_x$. Moreover, when we assume that $\phi_{\beta,x}$ is locally Lipschitz over Ω_x , the results in [44] ensure that for any $\varepsilon > 0$, choosing $N_\beta = \mathcal{O}(1/\varepsilon^2)$ guarantees that $\tilde{\beta}_x^* \geq \tilde{\beta}_x - \varepsilon$ with probability at least $\frac{3}{4}$.

Remark 2 As demonstrated in Definition 4, the penalty parameter $\tilde{\beta}_x$ is defined in the neighborhood Ω_x for any given reference point $x \in \mathcal{M}$. Therefore, the theoretical threshold value $\tilde{\beta}_x$ is guaranteed to be effective only in a neighborhood of the reference point \tilde{x} . For those cases where \mathcal{M} is a compact manifold, we can choose δ_β to be sufficiently large so that $\mathcal{M} \subset \mathcal{B}(\tilde{x}, \delta_\beta)$. Therefore, with $\beta > \tilde{\beta}_x^*$, we can conclude that there exists a neighborhood of \mathcal{M} , where CDF and OCP have the same first-order and second-order stationary points. Furthermore, in a wide range of popular optimization methods, the function value sequence of the generated iterates is non-increasing. That is, when we further assume the coercivity of the objective function f , there exists $M_x > 0$ such that the sequence $\{x_k\}$ is restricted within $\mathcal{B}(0, M_x)$. Under such settings, we can choose δ_β to enforce the equivalence between CDF and OCP in a neighborhood of $\mathcal{M} \cap \mathcal{B}(0, M_x)$.

3.3 Relationships between OCP and CDF

This subsection investigates the relationships between OCP and CDF on their stationary points and local minimizers. We start by presenting the explicit expression for the gradient and Hessian of CDF.

Proposition 5 The gradient of h in CDF can be expressed as

$$\nabla h(x) = J_{\mathcal{A}}(x) \nabla f(\mathcal{A}(x)) + \beta J_c(x) c(x). \quad (23)$$

Furthermore, under Assumption 3, the Hessian of $g(x) := f(\mathcal{A}(x))$ can be expressed as

$$\nabla^2 g(x) = J_{\mathcal{A}}(x) \nabla^2 f(\mathcal{A}(x)) J_{\mathcal{A}}(x)^\top + \mathcal{D}_{J_{\mathcal{A}}}(x) [\nabla f(\mathcal{A}(x))]. \quad (24)$$

and the Hessian of $h(x)$ is

$$\nabla^2 h(x) = \nabla^2 g(x) + \beta (J_c(x) J_c(x)^\top + \mathcal{D}_{J_c}(x) [c(x)]). \quad (25)$$

The proof for Proposition 5 is straightforward from the expression of h in CDF, hence we omit it for simplicity.

Proposition 6 *For any $x \in \mathcal{M}$, x is a first-order stationary point of OCP if and only if x is a first-order stationary point of CDF.*

Proof For any first-order stationary point, $x \in \mathcal{M}$ of OCP, it follows from the equality (2) that

$$\nabla h(x) = J_{\mathcal{A}}(x) \nabla f(x) + \beta J_c(x) c(x) = J_{\mathcal{A}}(x) J_c(x) \lambda(x) = 0,$$

which implies that x is a first-order stationary point of CDF.

On the other hand, for any $x \in \mathcal{M}$ that is a first-order stationary point of CDF, it holds that

$$J_{\mathcal{A}}(x) \nabla f(x) = 0,$$

which results in the inclusion $\nabla f(x) \in \mathcal{N}_x = \text{range}(J_c(x))$ from Lemma 7. By Definition 1, we conclude that x is a first-order stationary point of OCP.

Theorem 1 *For any given $x \in \mathcal{M}$, suppose $\beta > \tilde{\beta}_x$, then any first-order stationary point of CDF in Ω_x is a first-order stationary point of OCP.*

Proof For any $y \in \Omega_x$ that is a first-order stationary point of CDF, it holds from Proposition 5 that

$$0 = (y - \mathcal{A}(y))^\top \nabla h(y) = (y - \mathcal{A}(y))^\top J_{\mathcal{A}}(y) \nabla f(\mathcal{A}(y)) + \beta (y - \mathcal{A}(y))^\top J_c(y) c(y). \quad (26)$$

Moreover, from Definition 4, it holds that

$$(y - \mathcal{A}(y))^\top J_{\mathcal{A}}(y) \nabla f(\mathcal{A}(y)) \geq -\tilde{\beta}_x (y - \mathcal{A}(y))^\top J_c(y) c(y). \quad (27)$$

Note that we have used the fact that $(y - \mathcal{A}(y))^\top J_c(y) c(y) \geq 0$ from the proof of Proposition 4. Therefore, combined with (19), we obtain

$$\begin{aligned} 0 &= (y - \mathcal{A}(y))^\top J_{\mathcal{A}}(y) \nabla f(\mathcal{A}(y)) + \beta (y - \mathcal{A}(y))^\top J_c(y) c(y) \\ &\geq -\tilde{\beta}_x (y - \mathcal{A}(y))^\top J_c(y) c(y) + \beta (y - \mathcal{A}(y))^\top J_c(y) c(y) \\ &\geq \frac{\sigma_{x,c}(\beta - \tilde{\beta}_x)}{4M_{x,c}} \|c(y)\|^2, \end{aligned} \quad (28)$$

which illustrates that $\|c(y)\| = 0$ and thus $y \in \mathcal{M}$. Together with Proposition 6, we conclude that y is a first-order stationary point of OCP, and the proof is completed.

Theorem 2 *Suppose Assumption 3 holds. Then for any given $x \in \mathcal{M}$ with $\beta \geq \hat{\beta}_x$ in CDF, OCP and CDF have the same second-order stationary point over Ω_x .*

Proof For the first part of the proof, we aim to show that under Assumption 3, any second-order stationary point of CDF is a second-order stationary point of OCP. For any $y \in \Omega_x$ that is a second-order stationary point of CDF, y is also a first-order stationary point of CDF. Then based on Theorem 1, y is a first-order stationary point of OCP, and it holds that $y \in \mathcal{M}$. Then from Lemma 6, $J_{\mathcal{A}}(y)^\top d = d$ holds for any $d \in \mathcal{T}_y$, which implies the equality

$$d^\top \nabla^2 h(y) d = d^\top \left(\nabla^2 f(y) - \sum_{i=1}^p \lambda_i(y) \nabla^2 c_i(y) \right) d + d^\top (\mathcal{D}_{J_{\mathcal{A}}}(y)[\text{grad } f(y)]) d.$$

Since $y \in \mathcal{M}$ is a first-order stationary point of OCP, we have that $\text{grad } f(y) = 0$. Hence together with Proposition 2, we obtain the follow inequality,

$$\begin{aligned} \lambda_{\min}(\text{hess } f(y)) &\geq \min_{d \in \mathcal{T}_y, \|d\|=1} d^\top \nabla^2 h(y) d \geq \lambda_{\min}(\nabla^2 g(y)) \\ &= \lambda_{\min}(\nabla^2 h(y)) \geq 0. \end{aligned}$$

Therefore, we can conclude that y is a second-order stationary point of OCP. This completes the first part of the proof.

We prove the second part of this theorem by contradiction. Suppose x is a second-order stationary point of OCP but is not a second-order stationary point for CDF. Then there exists a constant $\tau > 0$ and a sequence $\{y_i\} \subset \Omega_x$ such that $\{y_i\} \rightarrow x$ and $h(y_i) < h(x) - \tau \|y_i - x\|^2$ holds for any $i \geq 0$.

From the inequality

$$\beta \geq 2 \cdot \sup_{y \in \Omega_x} \left\{ \max \left\{ \frac{2(f(\mathcal{A}^2(y)) - f(\mathcal{A}(y)))}{\|c(y)\|^2 - \|c(\mathcal{A}(y))\|^2}, 0 \right\} \right\},$$

it is easy to verify that the following inequality holds for any $y \in \Omega_x$,

$$h(\mathcal{A}(y)) = f(\mathcal{A}^2(y)) + \frac{\beta}{2} \|c(\mathcal{A}(y))\|^2 \leq f(\mathcal{A}(y)) + \frac{\beta}{2} \|c(y)\|^2 = h(y). \quad (29)$$

From (29), for any $i \geq 0$, it holds that

$$f(\mathcal{A}^\infty(y_i)) = h(\mathcal{A}^\infty(y_i)) \leq h(\mathcal{A}(y_i)) \leq h(y_i) < h(x) - \tau \|y_i - x\|^2. \quad (30)$$

Furthermore, notice that

$$\|\mathcal{A}^\infty(y_i) - y_i\| \leq \frac{4(M_{x,\mathcal{A}} + 1)}{\sigma_{x,c}} \|c(y_i)\|, \quad (31)$$

then it holds that

$$\begin{aligned}
\|\mathcal{A}^\infty(y_i) - x\| &\leq \frac{4(M_{x,A} + 1)}{\sigma_{x,c}} \|c(y_i)\| + \|y_i - x\| \\
&\leq \frac{4(M_{x,A} + 1)L_{x,c}}{\sigma_{x,c}} \text{dist}(y_i, \mathcal{M}) + \|y_i - x\| \\
&\leq \left(\frac{4(M_{x,A} + 1)L_{x,c}}{\sigma_{x,c}} + 1 \right) \|y_i - x\|.
\end{aligned} \tag{32}$$

Therefore, from (30), it holds that $\{\mathcal{A}^\infty(y_i)\} \rightarrow x$ and for any $i \geq 0$,

$$f(\mathcal{A}^\infty(y_i)) \leq f(x) - \frac{\tau}{\left(\frac{4(M_{x,A} + 1)L_{x,c}}{\sigma_{x,c}} + 1 \right)^2} \|\mathcal{A}^\infty(y_i) - x\|^2,$$

which contradicts the fact that x is a second-order stationary point of OCP as illustrated in [4, Proposition 5.5.5]. Therefore, from the contradiction, we can conclude that x is a second-order stationary point for CDF. This completes the entire proof.

4 Software Description

In this section, we give a brief overview of the structure of CDOpt. The idea behind the design for CDOpt is to guarantee the ease-of-use features for various types of users, including the users from optimization communities for solving standard Riemannian optimization problems over commonly used manifolds, the users from machine learning communities who wish to train neural networks with manifold constraints, and developers who aim to develop new manifolds and introduce more advanced features for CDOpt. As illustrated in Figure 1, we organize the CDOpt package into the following three parts:

- The manifold classes;
- The problem classes;
- The neural layers.

These three parts are mutually separated, hence it is easy to add new manifolds, and new neural layers in CDOpt with maximum code reuse for developers.

4.1 The manifold classes

The module “`manifold`” in CDOpt describes the manifold constraints by the following essential components for describing the corresponding constraint dissolving mapping,

- The expression of constraints $c(x)$, $J_c(x)$ and the Hessian-vector product of $\|c(x)\|^2$;

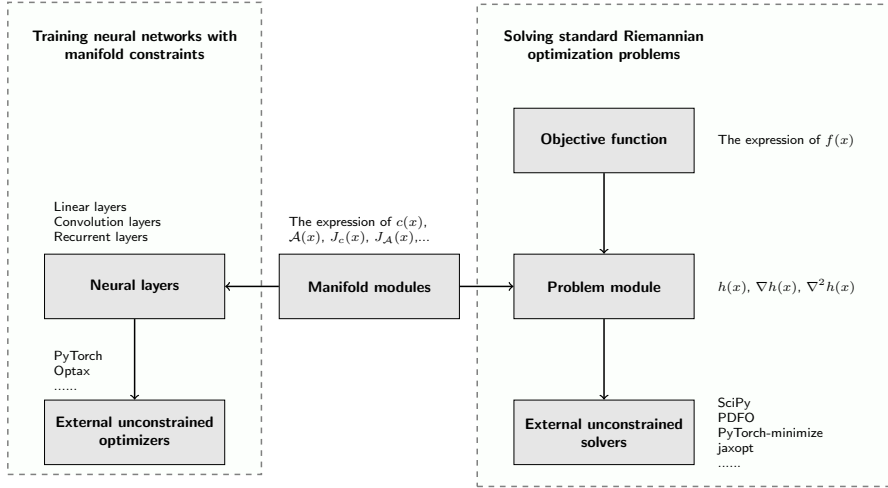


Fig. 1: The sketch of the structure of CDOpt.

- The expression of $\mathcal{A}(x)$, $J_{\mathcal{A}}(x)$ and the second-order differential of $\mathcal{A}(x)$;
- The rules to compute $h(x)$, $\nabla h(x)$, and $\nabla^2 h(x)$ from f , \mathcal{A} , c and their derivatives.

All the manifolds in CDOpt are available as derived classes from the base class named `basic_manifold`, which is available in the `manifold` module of CDOpt. Note that all the essential components in these manifold classes can be expressed by $c(x)$, $\mathcal{A}(x)$ and their differentials. Therefore, if some of these materials are not provided in the derived classes of the `basic_manifold`, all the essential materials can be automatically calculated based on the selected automatic differentiation (AD) packages from the supported numerical backends. In particular, if only the expression of $c(x)$ is provided in the derived class of `basic_manifold`, the constraint dissolving mapping is automatically chosen as

$$\mathcal{A}_c(x) = x - J_c(x)(J_c(x)^\top J_c(x) + \sigma \|c(x)\|^2 I_p)^\dagger c(x). \quad (33)$$

Here $J_c(x) \in \mathbb{R}^{n \times p}$ denotes the transpose of the Jacobian of c at x , which is also computed by the selected AD packages if it is not provided. Moreover, it is easy to verify that \mathcal{A}_c is locally Lipschitz over \mathbb{R}^n when J_c is locally Lipschitz smooth over \mathbb{R}^n . As a result, users only need to provide the expression of the manifold constraints $c(x)$ and its corresponding numerical backends for defining new manifold constraints through `basic_manifold` from the `manifold` module in CDOpt.

```
class customized_manifold(basic_manifold_np):
def __init__(self, var_shape, T):
m, s = *var_shape
self.T = T
self.I_s = np.eye(s)
super().__init__('customized_manifold', (m, s), (s, s))
```

```
def c(self, X):
    return (X.T @ X)@ self.T - self.Is
```

Listing 1: Define customized Riemannian manifold in CDOpt

CDOpt supports various numerical backends, where the type of the variables, APIs for build-in functions, and AD packages differ among different numerical backends. As a result, CDOpt provides some derived classes from `basic_manifold`: `basic_manifold_np`, `basic_manifold_torch` and `basic_manifold_jax`. In these derived classes, only the expression of $c(x)$ is required in defining a manifold, and their numerical backends are fixed as NumPy + Auto-grad, PyTorch and JAX, respectively. Then various specific manifolds, with different numerical backends, are developed by inheriting `basic_manifold_np`, `basic_manifold_torch` or `basic_manifold_jax`. Listing 1 illustrates how to define the Riemannian manifold $\{X \in \mathbb{R}^{m \times s} : X^\top X T = I_s\}$ in CDOpt only by the expression of the constraints $X^\top X T - I_s = 0$.

Furthermore, CDOpt provides various predefined manifolds, where the essential components are prefixed manually to achieve the best computational efficiency. Table 1 illustrates these predefined manifolds in CDOpt. Moreover, the formulation of their corresponding constraint dissolving mappings in CDOpt is listed in Table 2.

Remark 3 *In CDOpt, each point on the Grassmann manifold is an s -dimensional subspace embedded in \mathbb{R}^m and represented by an orthogonal $m \times s$ matrix. Consequently, optimization problems over the Grassmann manifold in CDOpt are treated as a specific class of optimization problems over the Stiefel manifold. Since the constraint dissolving mapping \mathcal{A} only depends on the constraints, the constraint dissolving mapping \mathcal{A} for the Grassmann manifold in CDOpt shares the same expression as that for the Stiefel manifold [63, 64].*

Additionally, compared to optimization problems over the Stiefel manifold in CDOpt, those over the Grassmann manifold require the objective functions to be orthogonally invariant. That is, for an objective function $f : \mathbb{R}^{m \times s} \rightarrow \mathbb{R}$, the equality $f(X) = f(XQ)$ holds for any $X \in \mathbb{R}^{m \times s}$ and any orthogonal matrix $Q \in \mathbb{R}^{s \times s}$. In contrast, the optimization problems over the Stiefel manifold admit more general functions. This leads to the different solution properties between these two classes of problems in CDOpt.

4.2 Problem class

The `problem` class in CDOpt describes the Riemannian optimization problem OCP by the manifold class for the constraints $c(x)$, the objective function $f(x)$ and its derivatives. As shown in Listing 2, CDOpt allows users to describe the optimization problem only from the expression of the objective function and the instantiated manifold.

```
manifold = stiefel_torch( (100,10) )
prob = cdopt.core.problem(manifold, obj_fun, beta = 'auto')
```

Listing 2: Describe Riemannian optimization problem in CDOpt

Table 1: Predefined manifold in CDOpt. Here $\mathbf{0}_{m \times m}$ denotes the $m \times m$ zero matrix, and X^H denotes the conjugate transpose of a complex matrix X .

Name	\mathcal{M}	Predefined manifolds
Euclidean space	\mathbb{R}^n	euclidean_np euclidean_torch euclidean_jax
Sphere	$\{x \in \mathbb{R}^n : \ x\ = 1\}$	sphere_np sphere_torch sphere_jax
Oblique manifold	$\{X \in \mathbb{R}^{m \times s} : \text{Diag}(XX^T) = I_m\}$	oblique_np oblique_torch oblique_jax
Stiefel manifold	$\{X \in \mathbb{R}^{m \times s} : X^T X = I_s\}$	stiefel_np stiefel_torch stiefel_jax
Grassmann manifold	$\{\text{range}(X) : X \in \mathbb{R}^{m \times s}, X^T X = I_s\}$	grassmann_np grassmann_torch grassmann_jax
Generalized Stiefel manifold	$\{X \in \mathbb{R}^{m \times s} : X^T B X = I_s, B \succeq 0\}$	generalized_stiefel_np generalized_stiefel_torch generalized_stiefel_jax
Hyperbolic manifold	$\{X \in \mathbb{R}^{m \times s} : X^T B X = I_s, B \text{ is indefinite}\}$	hyperbolic_np hyperbolic_torch hyperbolic_jax
Symplectic Stiefel manifold	$\{X \in \mathbb{R}^{2m \times 2s} : X^T Q_m X = Q_s, Q_m := \begin{bmatrix} \mathbf{0}_{m \times m} & I_m \\ -I_m & \mathbf{0}_{m \times m} \end{bmatrix}\}$	symp_stiefel_np symp_stiefel_torch symp_stiefel_jax
Stiefel manifold with range constraint	$\{X \in \mathbb{R}^{m \times s} : X^T X = I_s, X X^T e = e, \ e\ = 1\}$	stiefel_range_constraints_np stiefel_range_constraints_torch stiefel_range_constraints_jax
Complex sphere	$\{x \in \mathbb{C}^n : \ x\ = 1\}$	complex_sphere_np complex_sphere_torch complex_sphere_jax
Complex oblique manifold	$\{X \in \mathbb{C}^{m \times s} : \text{Diag}(X X^H) = I_m\}$	complex_oblique_np complex_oblique_torch complex_oblique_jax
Complex Stiefel manifold	$\{X \in \mathbb{C}^{m \times s} : X^H X = I_s\}$	complex_stiefel_np complex_stiefel_torch complex_stiefel_jax
Product manifold	$\mathcal{M}_1 \times \mathcal{M}_2 \times \dots$	product_manifold

Table 2: Default implementations of the constraint dissolving mappings \mathcal{A} for the predefined Riemannian manifolds in CDOpt. Here $\mathbf{0}_{m \times m}$ denotes the $m \times m$ zero matrix, and X^H denotes the conjugate transpose of a complex matrix X .

Name of the manifold	Expression of \mathcal{M}	Default choice of \mathcal{A} in CDOpt
Euclidean space	$\{x : x \in \mathbb{R}^n\}$	$x \mapsto x$
Sphere	$\{x \in \mathbb{R}^n : \ x\ = 1\}$	$x \mapsto 2x/(1 + \ x\ _2^2)$ [64]
Oblique manifold	$\{X \in \mathbb{R}^{m \times s} : \text{Diag}(X X^T) = I_m\}$	$X \mapsto 2(I_m + \text{Diag}(X X^T))^{-1} X$ [64]
Stiefel manifold	$\{X \in \mathbb{R}^{m \times s} : X^T X = I_s\}$	$X \mapsto X(\frac{3}{2}I_s - \frac{1}{2}X^T X)$ [63]
Grassmann manifold	$\{\text{range}(X) : X \in \mathbb{R}^{m \times s}, X^T X = I_s\}$	$X \mapsto X(\frac{3}{2}I_s - \frac{1}{2}X^T X)$ [64]
Generalized Stiefel manifold	$\{X \in \mathbb{R}^{m \times s} : X^T B X = I_s\}$ for some positive definite B	$X \mapsto X(\frac{3}{2}I_s - \frac{1}{2}X^T B X)$ [64]
Hyperbolic manifold [7]	$\{X \in \mathbb{R}^{m \times s} : X^T B X = I_s\}$ for some B that satisfies $\lambda_{\min}(B) < 0 < \lambda_{\max}(B)$	$X \mapsto X(\frac{3}{2}I_s - \frac{1}{2}X^T B X)$ [64]
Symplectic Stiefel manifold [54]	$\{X \in \mathbb{R}^{2m \times 2s} : X^T Q_m X = Q_s, Q_m := \begin{bmatrix} \mathbf{0}_{m \times m} & I_m \\ -I_m & \mathbf{0}_{m \times m} \end{bmatrix}\}$	$X \mapsto X(\frac{3}{2}I_{2s} + \frac{1}{2}Q_s X^T Q_m X)$ [64]
Stiefel manifold with range constraint [35]	$\{X \in \mathbb{R}^{m \times s} : X^T X = I_s, X X^T e = e\}$ for some $e \in \mathbb{R}^m$ such that $\ e\ = 1$.	$X \mapsto X(\frac{3}{2}I_s - \frac{1}{2}X^T X + (X^T X - 2I_s)X^T e e^T X) + e e^T X$
Complex sphere	$\{x \in \mathbb{C}^n : \ x\ = 1\}$	$x \mapsto 2x/(1 + \ x\ _2^2)$
Complex oblique manifold	$\{X \in \mathbb{C}^{m \times s} : \text{Diag}(X X^H) = I_m\}$	$X \mapsto 2(I_m + \text{Diag}(X X^T))^{-1} X$
Complex Stiefel manifold	$\{X \in \mathbb{C}^{m \times s} : X^H X = I_s\}$	$X \mapsto X(\frac{3}{2}I_s - \frac{1}{2}X^H X)$ [64]

When instantiating the `problem` class, the argument `obj_fun` should be a callable object, and the argument `manifold` should be the instantiation of the `manifold` class in CDOpt. Other materials for optimization, including the gradient and Hessian of the objective function f , are optional in the instantiation of `problem` class. If these materials are not provided, the `problem` class automatically computes them by the chosen numerical backends behind the interface.

Furthermore, if the penalty parameter β in CDF is not provided in the instantiation of the `problem` class, CDOpt can automatically estimate an appropriate value of β . When the argument `beta` is set as 'auto', CDOpt randomly chooses the penalty parameter by the scheme presented in Remark 1, where the reference point $\tilde{x} \in \mathcal{M}$ from the `Init_point` method of the `manifold`

class, and the default values for the hyperparameters are chosen as $N_\beta = 100$, $\delta_\beta = 0.01$, $\varepsilon_\beta = 10^{-14}$ and $\theta_\beta = 2$. Users can set their customized hyperparameters via the argument `autobeta_args`.

After instantiation, the `problem` class provides the constraint dissolving function CDF and its derivatives as callable objects. In the attributes of the `problem` class, `cdf_obj`, `cdf_grad` and `cdf_hvp` are callable objects that return the function value, gradient and Hessian-vector product of the constraint dissolving function, respectively. Their input arguments and outputs are of the same type as the selected numerical backend of the problem. Moreover, to adapt the optimizers that are developed based on NumPy and SciPy, the `problem` class provides the attributes `cdf_obj_vec_np`, `cdf_grad_vec_np` and `cdf_hvp_vec_np`, where their inputs and outputs are all NumPy 1D array. Based on the provided attributes from the `problem` class, users can directly apply the unconstrained optimization solvers from various existing packages, such as SciPy, PDFO, PyTorch-minimize and jaxopt.

4.3 Neural layers

PyTorch and Flax are powerful frameworks for training neural networks, where neural networks are built by neural layers from `torch.nn` or `flax.linen` modules. For those users that aim to train neural networks with manifold constraints, CDOpt provides various predefined neural layers in its `cdopt.nn` and `cdopt.linen` modules for PyTorch and Flax, respectively. These predefined layers in CDOpt preserve the same APIs as the layers from PyTorch and Flax, hence users can plug these layers into the neural networks with minimal modification to the standard PyTorch or Flax codes.

The neural layers from `cdopt.nn` module are the derived classes of the `module` class from `torch.nn`, hence can be integrated with any neural network built from the neural layers from `torch.nn`. Therefore, users can build neural networks by mixing the layers from both `cdopt.nn` and `torch.nn`. In the instantiation of the neural layers from `cdopt.nn`, users can set the manifold constraints by the `manifold_class` argument and choose the penalty parameter β by the `penalty_param` argument. When instantiated, the neural layers in the `cdopt.nn` module first call its `__init__` method to instantiate the manifold according to the `manifold_class` argument and generate the initial weights on the manifold. After instantiation, the neural layers provide the attributes `manifold` and `quad_penalty` to access the instantiated manifolds and the value of $\|c(x)\|^2$, respectively. Moreover, for any neural network that is built from the neural layers from `cdopt.nn` and `torch.nn`, we can call the function `get_quad_penalty()` from `cdopt.nn` to compute the sum of all the quadratic penalty terms of its neural layers from `cdopt.nn`.

Currently, CDOpt implements the following neural layers for PyTorch in the `cdopt.nn` module,

- `Linear`, `Bilinear`, `LazyLinear`;
- `Conv1d`, `Conv2d`, `Conv3d`;

- ConvTranspose1d, ConvTranspose2d, ConvTranspose3d;
- RNN, LSTM, GRU, RNNCell, LSTMCell, GRUCell.

Listing 3 presents a simple example, where we build a two-layer neural network by the layers from `CDOpt.nn` and `PyTorch.nn`.

```
class Net(nn.Module):
def __init__(self):
super(Net, self).__init__()
self.conv = Conv2d_cdopt(1, 6, 5,
manifold_class=stiefel_torch, penalty_param = 0.05)
self.fc = nn.Linear(84, 10)

def forward(self, x):
x = F.max_pool2d(F.relu(self.conv(x)), (2, 2))
x = self.fc(x)
x = F.log_softmax(x, dim=1)
return x
```

Listing 3: Building a two-layer neural network with manifold constraints in PyTorch by predefined neural layers from `cdopt.nn`.

Furthermore, for those neural layers that are not available from `cdopt.nn`, CDOpt provides a simple way to add manifold constraints to the parameters of these neural layers. Through the function `set_constraint_dissolving` from `cdopt.nn.utils.set_constraints`, users can set the manifold constraints to the neural layers by just providing the neural layers, the name of target parameters, and the manifold class. Listing 4 presents a simple example on how to set the manifold constraints for the weights in a two-layer neural network.

```
class Net(nn.Module):
def __init__(self):
super(Net, self).__init__()
self.conv = nn.Conv2d(1, 6, 5)
self.fc = nn.Linear(84, 10)
set_constraint_dissolving(self.conv, 'weight',
manifold_class=stiefel_torch, penalty_param = 0.05)

def forward(self, x):
x = F.max_pool2d(F.relu(self.conv(x)), (2, 2))
x = self.fc(x)
x = F.log_softmax(x, dim=1)
return x
```

Listing 4: Building a two-layer neural network with manifold constraints in PyTorch by the function `set_constraint_dissolving` from `cdopt.nn.utils.set_constraints`.

For Flax, CDOpt implements the following neural layers for training neural networks,

- Dense, DenseGeneral;
- Conv, ConvTranspose.

It is worth mentioning that the neural layers in Flax are designed in a different way from those in `PyTorch.nn`. In Flax, the neural layers are separated from their weights and behave as functions that map the inputs and weights to their outputs by the `__call__` method. As a result, although the neural layers from `linen` module can be called by the same arguments as those from `Flax.linen`, the quadratic penalty term $\|c(x)\|^2$ is returned by the `__call__` method. Listing 5 illustrates how to build a neural network by the neural layers from `CDOpt.linen` and `Flax.linen`.

```

class model(flax.linen.Module):
    @flax.linen.compact
    def __call__(self, x):
        x, quad_penalty = cdopt.linen.Conv_cdopt(features=32, kernel_size=(3, 3),
        manifold_class = stiefel_jax)(x)
        x = flax.linen.relu(x)
        x = flax.linen.avg_pool(x, window_shape=(2, 2), strides=(2, 2))
        x = flax.linen.Dense(features=10)(x)
        return x, quad_penalty

```

Listing 5: Building a two-layer neural network with manifold constraints in Flax by predefined neural layers from `cdopt.linen`

4.4 Optimization through CDOpt

In CDOpt, the Riemannian optimization problem OCP is transformed into the unconstrained minimization of the constraint dissolving function CDF. Therefore, various existing unconstrained optimization solvers can be directly applied to solve OCP through minimizing CDF. CDOpt only requires the following steps for solving the optimization problem through the `problem` class,

1. Define the objective function $f : \mathbb{R}^n \rightarrow \mathbb{R}$;
2. Instantiation of the manifold $\mathcal{M} = \{x \in \mathbb{R}^n : c(x) = 0\}$;
3. Describe the optimization problem through `problem` class;
4. Call an external solver to minimize the constraint dissolving function.

As far as we tested, CDOpt supports the following solvers from SciPy, PDFO [52], PyTorch-minimize [18], and jaxopt [10],

- SciPy: CG, BFGS, Newton-CG, L-BFGS-B, TNC, `trust-ncg`, and `trust-krylov`;
- PyTorch-minimize: CG, L-BFGS, `trust-ncg`, and `trust-krylov`;
- jaxopt: GradientDescent, LBFGS, NonlinearCG, and its interface for the package `scipy.optimize.minimize`;
- PDFO: `newuoa`, `bobyqa`, `lincoa`.

On the other hand, CDOpt provides simple approaches to build and train neural networks that invoke manifold constraints. To impose manifold constraints to the weights of a neural layer, users only need the following two steps,

1. Replace that neural layer with its corresponding neural layers from `cdopt.nn` and `cdopt.linen`;
2. Add the quadratic penalty terms to the loss function in the training process.

Then various unconstrained optimizers (i.e. solvers for training neural networks) can be directly applied to train the modified neural network. Currently, CDOpt is tested to successfully support the following optimizers,

- All the optimizers from PyTorch and PyTorch-optimizer;
- All the optimizers from Optax.

5 Comparison with Existing Packages

In this section, we present a brief comparison between CDOpt and existing Python Riemannian optimization packages, including PyManopt, Geoopt, McTorch and GeoTorch. The major difference between CDOpt and these existing packages is how the OCP is treated. Developed from constraint dissolving approaches, CDOpt transfers OCP into the unconstrained minimization of CDF, where the construction of CDF avoids the need of geometrical materials from differential geometry.

CDOpt only requires $c(x)$, $\mathcal{A}(x)$, and their derivatives to describe the Riemannian manifold, hence it provides great convenience in defining Riemannian manifolds. As demonstrated in [64], it is usually easy to design the constraint dissolving mapping \mathcal{A} for \mathcal{M} since the constraint dissolving mappings only need to satisfy Assumption 2. When only $c(x)$ is provided, we can choose the constraint dissolving mapping as in (33) with appropriate $\sigma \geq 0$. Due to the great convenience in describing the manifolds, CDOpt provides a wider range of pre-defined manifold classes than existing Riemannian optimization packages. Moreover, CDOpt enables users to define new manifolds only from the expression of the constraints, hence defining a new manifold in CDOpt is significantly easier than the existing Riemannian optimization packages. A detailed comparison of the supported manifolds and essential materials for new manifolds is presented in Table 3.

As CDOpt transforms OCP into the unconstrained minimization of the constraint dissolving function, CDOpt can directly and efficiently utilize existing unconstrained optimization solvers without modifying them to adapt the geometrical material. Currently, CDOpt is compatible with various existing unconstrained optimization solvers. For the optimization problem defined by the `problem` class, CDOpt can directly call all the solvers provided by SciPy, PyTorch-minimize, PDFO, jaxopt and various other unconstrained optimization packages. For training neural networks, CDOpt is compatible to the optimizers from PyTorch, PyTorch-optimizer, Optax, and various open-sourced optimizers. However, most existing Riemannian optimization packages have to develop specialized solvers to utilize the geometrical materials. Therefore, their supported solvers are relatively limited. Detailed comparisons are presented in Table 4.

Furthermore, as all of the existing Riemannian optimization packages require geometrical materials or specialized solvers, their supported numerical backends are also relatively limited. For example, although PyManopt supports PyTorch, Autograd and Tensorflow in its AD modules, its manifold module and solver module only support Numpy as the numerical backend. Additionally, the packages GeoTorch, Geoopt and McTorch are only developed based on PyTorch. As a comparison, CDOpt supports various of numerical backends in its modules, including the Numpy, PyTorch, JAX, etc. We present a detailed comparison in Table 5.

Table 3: Comparison of the compared packages in terms of manifold and necessary materials for defining a new manifold.

	CDOpt	Pymanopt	Geoopt	McTorch	GeoTorch
Euclidean space	✓	✓	✓	✓	✓
Sphere	✓	✓	✓	✓	✓
Oblique manifold	✓	✓	✗	✓	✗
Stiefel manifold	✓	✓	✓	✓	✓
Grassmann manifold	✓	✓	✓	✓	✓
Generalized Stiefel manifold	✓	✗	✗	✗	✗
Hyperbolic manifold	✓	✗	✗	✓	✗
Symplectic Stiefel manifold	✓	✗	✗	✗	✗
Complex sphere	✓	✓	✗	✗	✗
Complex oblique manifold	✓	✗	✗	✗	✗
Complex Stiefel manifold	✓	✗	✗	✗	✗
Product manifold	✓	✓	✓	✓	✓
Defining new manifolds	The expression of $c(x)$	Exponential and log-arithmetic maps, retraction, vector transport, egrad2rgrad, ehess2rhess, inner product, distance, norm	Exponential and log-arithmetic maps, retraction, vector transport, egrad2rgrad, ehess2rhess, inner product, distance, norm	Exponential and log-arithmetic maps, retraction, vector transport, egrad2rgrad, ehess2rhess, inner product, distance, norm	The explicit formation of a surjection from \mathbb{R}^N onto \mathcal{M} for some $N > 0$.

6 Examples

In this section, we briefly introduce the features of CDOpt through several illustrative examples. Interested readers can refer to https://cdopt.github.io/md_files/examples.html for more examples of applying CDOpt to solve Riemannian optimization problems.

6.1 Orthogonal dictionary learning

CDOpt is easy-to-use when it is employed to solve standard Riemannian optimization problems through its `problem` class. CDOpt integrates various numerical backends such as Autograd, PyTorch, and JAX. Various important features of these packages, including AD packages, GPU supports and JIT compilation, are performed behind CDOpt’s `problem` and `manifold` modules. Therefore, users are only required to provide a small amount of set-up codes for solving Riemannian optimization problems through CDOpt.

We briefly demonstrate the easy-to-use features of CDOpt by a simple example on orthogonal dictionary learning (ODL). Given data $\{y_i\}_{i=1,\dots,m}$ generated by $y_i = Qz_i$, where Q is a fixed unknown orthogonal matrix and each z_i follows an i.i.d. Bernoulli-Gaussian distribution with parameter $\theta \in (0, 1)$. ODL aims to recover the matrix $Z = [z_1, \dots, z_m] \in \mathbb{R}^{m \times n}$ and the orthogonal matrix $Q \in \mathbb{R}^{n \times n}$ from the given data $Y = [y_1, \dots, y_m]^T \in \mathbb{R}^{m \times n}$.

Based on the ℓ_4 -norm maximization model proposed in [29, 69], we consider the following optimization problem over the Stiefel manifold:

$$\begin{aligned}
 \min_{X=[x_1, \dots, x_n] \in \mathbb{R}^{n \times n}} \quad & f(X) := \sum_{1 \leq i \leq m, 1 \leq j \leq n} -(y_i^\top x_j)^4 \\
 \text{s. t.} \quad & X^T X = I_n.
 \end{aligned} \tag{34}$$

Table 4: Comparison of available solvers in general optimization (the optimization tasks defined by derivatives of the objective functions and manifolds), and training neural network via PyTorch.

	CDopt	Pymanopt	Geoopt	McTorch	GeoTorch
Derivate-free solvers	NEWUOA, BOBYQA, LINCOA from PDFO	N.A.	N.A.	N.A.	N.A.
First-order solvers	Conjugate gradient, BFGS, limit-memory BFGS from SciPy, PyTorch-minimize and jaxopt	Riemannian conjugate gradient, Riemannian steepest descent, Riemannian line-search.	N.A.	N.A.	N.A.
Second-order solvers	Newton-CG, truncated Newton, trust-region with Krylov subsolver, trust-region Newton-CG from SciPy and PyTorch-minimize	Riemannian trust-region	N.A.	N.A.	N.A.
Training in PyTorch	All the optimizers from PyTorch.optim and PyTorch-optimizer	N.A.	Riemannian Adam, Riemannian line-search, Riemannian SGD	Riemannian Adagrad, Riemannian SGD	All the optimizers from PyTorch.optim and PyTorch-optimizer
Training in JAX	All the optimizers from Optax	N.A.	N.A.	N.A.	N.A.

Table 5: Comparison of the supported backends in different components of the compared packages.

	CDopt	Pymanopt	Geoopt	McTorch	GeoTorch
Automatic differentiation	Autograd, PyTorch, JAX	Autograd, PyTorch, TensorFlow, Theano	PyTorch	PyTorch	PyTorch
Manifold	NumPy, SciPy, PyTorch, JAX	NumPy, SciPy	PyTorch	PyTorch	PyTorch
Optimization	SciPy, PyTorch, JAX, Optax	NumPy	PyTorch	PyTorch	PyTorch

The following script demonstrates how to solve (34) through CDOpt and JAX:

```
import numpy as np
import scipy as sp
import jax
import jax.numpy as jnp
import cdopt
from cdopt.manifold_jax import stiefel_jax

# Generating the data
n = 30
m = 10*n**2
theta = 0.3

# Set jax device and data type
device = jax.devices('gpu')[0]

Q, R = np.linalg.qr(np.random.randn(n,n))
Y = jax.device_put(jnp.array(
    ((np.random.rand(m,n)) * (np.random.rand(m,n) <= theta)) @ Q), device)

# Define objective function and Stiefel manifold
def obj_fun(X):
    return -jnp.sum(jnp.matmul(Y, X) **4 )

M = stiefel_jax((n,n), device= device)

# Describe the optimization problem and set the penalty parameter \beta.
problem_test = cdopt.core.problem(M, obj_fun, beta = 'auto')

# The vectorized function value, gradient and Hessian-vector product
# of the constraint dissolving function.
cdf_fun_np = problem_test.cdf_fun_vec_np
cdf_grad_np = problem_test.cdf_grad_vec_np
cdf_hvp_np = problem_test.cdf_hvp_vec_np

## Apply limit memory BFGS solver from scipy.minimize
from scipy.optimize import fmin.bfgs, fmin.cg, fmin.l.bfgs.b, fmin.ncg

# optimize by L-BFGS method
out_msg = sp.optimize.minimize(cdf_fun_np, problem_test.Xinit_vec_np,
                              method='L-BFGS-B', jac = cdf_grad_np)
```

6.2 Training neural network with orthogonal weight normalization

In this subsection, we present a simple example of training VGG19 [53] with orthogonally constrained convolutional kernels. The following script further demonstrates that neural networks with manifold constraints can be easily defined and trained through CDOpt. Since all the neural layers from `cdopt.nn` have the same APIs as those from `torch.nn`, modifying a neural network to involve manifold constraints through CDOpt is simple and requires minimum modifications to the standard PyTorch codes.

```
import torch
import torch.nn as nn
import torch.optim as optim
import torch.nn.functional as F

import torchvision
import torchvision.transforms as transforms

import cdopt
from cdopt.nn import Conv2d_cdopt, get_quad_penalty
from cdopt.manifold_torch import stiefel_torch

cfg_vgg19 = [64, 64, 'M', 128, 128, 'M', 256, 256, 256, 256, 'M',
            512, 512, 512, 512, 'M', 512, 512, 512, 512, 'M']

class VGG(nn.Module):
    def __init__(self):
        super(VGG, self).__init__()
```

```

self.features= self._make_layers(cfg.vgg19)
self.classifier = nn.Sequential(
    nn.Linear(512 * 7 * 7, 4096),
    nn.ReLU(inplace=True),
    nn.Dropout(0.5),
    nn.Linear(4096, 4096),
    nn.ReLU(inplace=True),
    nn.Dropout(0.5),
    nn.Linear(4096, 10),
)
self.avgpool = nn.AdaptiveAvgPool2d(7)

def forward(self, x):
    out = self.features(x)
    out = self.avgpool(out)
    out = out.reshape(out.size(0), -1)
    out = self.classifier(out)
    return out

def _make_layers(self, cfg):
    layers = []
    in_channels = 3
    for x in cfg:
        if x == 'M':
            layers += [nn.MaxPool2d(kernel_size=2, stride=2)]
        else:
            local_block = [Conv2d_cdopt(in_channels, x, kernel_size=3,
                padding=1, manifold_class=stiefel_torch, penalty_param = 0.05),
                nn.BatchNorm2d(x), nn.ReLU(inplace=True)]
            layers += local_block
            in_channels = x
    layers += [nn.AvgPool2d(kernel_size=1, stride=1)]
    return nn.Sequential(*layers)

def train(model, device, train_loader, optimizer, epoch):
    model.train()
    for batch_idx, (data, target) in enumerate(train_loader):
        data, target = data.to(device), target.to(device)
        optimizer.zero_grad()
        output = model(data)
        # Add quadratic penalty terms to the loss function.
        loss = F.nll_loss(output, target) + get_quad_penalty(model)
        loss.backward()
        optimizer.step()

device = torch.device("cuda")
model = VGG().to(device)
optimizer = optim.Adam(model.parameters(), lr= 1e-3)
transform=transforms.Compose([ transforms.ToTensor(), ])
trainset = torchvision.datasets.CIFAR10(
    root='./data', train=True, download=True, transform=transform)
train_loader = torch.utils.data.DataLoader(trainset, batch_size=128,
    shuffle=True, pin_memory=True)

for epoch in range(100):
    train(model, device, train_loader, optimizer, epoch)

```

7 Numerical Experiments

In this section, we test the performance of CDOpt on several important applications of OCP. For standard Riemannian optimization problems, we compare the numerical performance of CDOpt with PyManopt (version 2.2.0). On the other hand, for training neural networks over Riemannian manifolds, we choose to use GeoTorch (version 0.3.0) and McTorch (version 0.1.0) in the comparison. All the experiments are performed on Ubuntu 20.02 platform with Intel Xeon 6342 and NVIDIA GeForce RTX 3090. Moreover, we run all these numerical experiments in Python 3.8.10 with NumPy 1.23, SciPy 1.8.1, PyTorch 1.9.0, CUDA 11.4 and JAX 0.3.14.

Remark 4 *It is worth mentioning that the limited memory BFGS (L-BFGS) and conjugate gradient (CG) solvers in SciPy package are implemented in*

FORTRAN and C++, respectively, hence exhibiting high computational efficiency. These two solvers are integrated into SciPy via F2PY interfaces. In contrast, all the solvers in PyManopt are developed entirely in Python.

This distinction highlights one of the major advantages of the CDOpt package: CDOpt admits direct implementations of highly efficient unconstrained solvers for Riemannian optimization problems. Nonetheless, due to the inherent differences in the implementation languages of the solvers in CDOpt and PyManopt, a direct comparison of CPU times might not be equitable for the solvers in PyManopt. Therefore, for better illustrations of the numerical performance of CDOpt, we report both the CPU time and the number of evaluations of function values and gradients in our numerical experiments.

7.1 Choices of different constraint dissolving mappings

Section 4.1 demonstrates that CDOpt includes several predefined well-established Riemannian manifolds. Additionally, CDOpt supports the customized definition for manifolds, which only requires the expression of the constraints function c . Then CDOpt automatically generates all other essential components using (33) and AD algorithms.

The predefined manifolds listed in Table (1) require only matrix-matrix multiplications to compute constraint dissolving mappings. In contrast, when employing \mathcal{A}_c from (33) as the constraint dissolving mapping, one must solve $p \times p$ linear equations to obtain $\mathcal{A}_c(x)$. Intuitively, for the predefined manifolds in Table (1), it is generally more computationally efficient to use the mappings listed in Table 2 rather than those determined by (33).

In this subsection, we aim to perform preliminary numerical experiments to evaluate the computational efficiency of these two different choices of constraint dissolving mappings in CDOpt. In our numerical experiments, we choose the sphere, Stiefel manifold, and symplectic Stiefel manifold for the comparison. For these manifolds, with a given randomly generated $x \in \mathbb{R}^n$, we measure the CPU time for computing the $\mathcal{A}(x)$, $J_{\mathcal{A}}(x)$, and $\mathcal{D}_{J_{\mathcal{A}}}(x)$ with respect to different choices of the constraint dissolving mappings from Table 2 and (33), respectively. Each test instance is replicated for 1000 times by using the built-in `timeit` module in Python, and we report the average CPU time in seconds.

Figure 2 shows the comparison of the computation time for different constraint dissolving mappings in CDOpt. From the curves in Figure 2, it can be inferred that the computational time for the mappings \mathcal{A} , $J_{\mathcal{A}}$, and $\mathcal{D}_{J_{\mathcal{A}}}$ in Table 2, is considerably shorter compared to the cases where \mathcal{A} is selected based on (33). Consequently, for any Riemannian optimization problem where the manifold is listed in Table 1, the predefined manifolds in CDOpt are recommended for better computational efficiency.

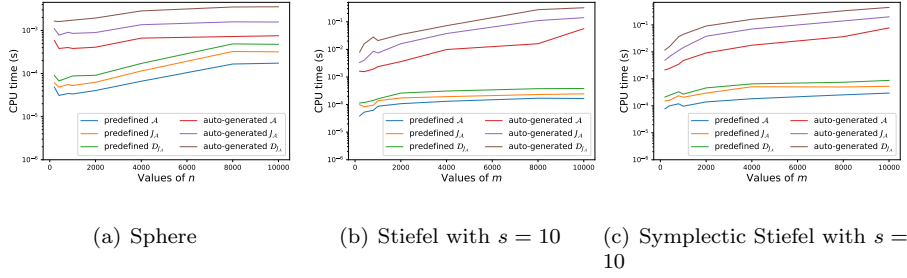


Fig. 2: Comparisons of the computational times for different choices of the constraint dissolving mappings in CDOpt. Here “predefined” refers to choosing \mathcal{A} as specified in Table 2, and “auto-generated” means choosing \mathcal{A} by (33).

7.2 Nearest correlation matrix

In this subsection, we test the numerical performance of CDOpt on optimization problems defined by its `problem` interface. Moreover, we compare CDOpt with the state-of-the-art Riemannian optimization package PyManopt (version 2.2.0), where the Riemannian optimization problems must be defined through its `problem` interface.

Our test example is the problem of finding the nearest low-rank correlation matrix (NCM) to a given matrix $G \in \mathbb{R}^{n \times p}$, which can be reshaped as an optimization problem over the oblique manifold

$$\begin{aligned} \min_{X \in \mathbb{R}^{n \times p}} \quad & f(X) = \frac{1}{2} \|H \circ (XX^\top - G)\|_F^2 \\ \text{s.t.} \quad & \text{Diag}(XX^\top) = I_n, \end{aligned} \quad (35)$$

where $H \in \mathbb{R}^{n \times n}$ is a nonnegative weight matrix. For all the numerical experiments in this subsection, we generate the matrix \hat{G} from the gene expression data provided in [41]¹. Then the matrix G is generated by perturbing \hat{G} by $G = (1 - \theta)\hat{G} + \theta E$, where $\theta \geq 0$ is a prefixed parameter, and $E \in \mathbb{R}^{n \times n}$ is a randomly generated matrix with all of its diagonal entry equals to 1. The weight matrix H in (35) is chosen as a symmetric matrix whose entries are uniformly distributed in $[0, 1]$.

We set the penalty parameter β for CDF by setting `beta = 'auto'` in the instantiation of the `problem` class in CDOpt. We choose the L-BFGS, CG and trust-region solvers from SciPy to test the numerical performance of CDOpt. For comparison, we choose the Riemannian CG solver and Riemannian trust-region solver from PyManopt since L-BFGS is not available in PyManopt. For CDOpt, we stop these solvers when the maximum number of iterations exceeds 10000 or the norm of the gradient its corresponding constraint dissolving function is less than 10^{-5} . For the solvers from PyManopt, we stop these solvers

¹ available at <https://blog.nus.edu.sg/mattohkc/files/2019/11/covseldata.zip>

once the norm of its Riemannian gradient is smaller than 10^{-5} , or the maximum number of iterations exceeds 10000. All the other parameters are fixed as their default values. Additionally, all the solvers start from the same initial point, which is randomly generated on the oblique manifold in each test instance.

Furthermore, we fix the numerical backends as the PyTorch package in both CDOpt and PyManopt. We only provide the expression of the objective function in all the test instances, thus the gradient and the Hessian of f are automatically computed by the AD packages from the PyTorch backends in CDOpt or PyManopt.

Table 7 – Table 10 report the numerical results on the comparison of CDOpt and PyManopt, where the detailed meanings of their column headers are presented in Table 6. It is worth mentioning that in PyManopt (version 2.2.0), the number of evaluations for gradients and Hessians is unavailable in its built-in Riemannian trust-region solver (pymanopt-rtr). Therefore, those entries are recorded as “None” in Table 7 - Table 10.

Table 6: The detailed meanings of the column headers in the tables that report the results of numerical experiments. Here x^* denoted the output of the solvers.

Abbreviation	Detailed meaning
fval	The value of $f(x^*)$
iter	Total number of iterations
eval_f	Total number of evaluations of the function values of f
eval_grad	Total number of evaluations of the gradients of f
stat	The ℓ_2 -norm of the Riemannian gradient of f at x^*
feas	The value of $\ c(x^*)\ $
time (s)	Total running time of the solver (in seconds)
acc	Test accuracy at the final epoch
time/epoch	The averaged running time (in seconds) per epoch

From Table 7 – Table 10, we can observe that CDOpt achieves comparable performance as PyManopt in all the numerical experiments. Moreover, although CDOpt needs to reshape the variables in each iteration, applying the conjugate gradient method and trust-region method from SciPy package shows superior performance over their Riemannian counterparts from PyManopt when p exceeds 100, particularly on GPU architectures. Furthermore, benefiting from the highly efficient L-BFGS solver that is programmed in FORTRAN and wrapped by the SciPy package, CDOpt gains significant advantages against the compared Riemannian solvers from PyManopt. These numerical results indicate the great potential of our developed CDOpt package.

Table 7: Nearest correlation matrix problem on the ER dataset on CPUs.

		fval	iter	eval_f	eval_grad	stat	feas	time (s)
$p = 10$	cdopt-lbfgs	2.30e+03	178	188	188	9.93e-06	4.50e-15	0.63
	cdopt-cg	2.30e+03	238	363	363	9.26e-06	4.29e-15	0.96
	cdopt-tr	2.30e+03	75	76	71	7.88e-06	4.35e-15	4.06
	pymanopt-rcg	2.30e+03	314	314	314	9.56e-06	5.42e-15	0.74
	pymanopt-rtr	2.30e+03	41	None	None	2.75e-06	5.54e-15	1.42
$p = 20$	cdopt-lbfgs	7.69e+02	196	205	205	8.79e-06	4.62e-15	0.83
	cdopt-cg	7.69e+02	250	388	388	9.44e-06	2.78e-13	7.56
	cdopt-tr	7.69e+02	63	64	58	2.54e-07	3.92e-15	40.37
	pymanopt-rcg	7.69e+02	301	301	301	8.66e-06	6.01e-15	6.40
	pymanopt-rtr	7.69e+02	26	None	None	3.02e-08	6.14e-15	10.38
$p = 30$	cdopt-lbfgs	4.27e+02	323	337	337	8.45e-06	3.55e-15	2.03
	cdopt-cg	4.27e+02	732	1089	1089	8.22e-06	5.63e-15	24.95
	cdopt-tr	4.27e+02	73	74	66	9.48e-06	4.88e-15	36.32
	pymanopt-rcg	4.27e+02	599	599	599	7.01e-06	5.58e-15	12.24
	pymanopt-rtr	4.27e+02	31	None	None	1.64e-07	6.45e-15	29.63
$p = 50$	cdopt-lbfgs	2.34e+02	428	445	445	7.97e-06	4.61e-13	4.86
	cdopt-cg	2.34e+02	732	1107	1107	6.31e-06	4.09e-15	26.19
	cdopt-tr	2.34e+02	59	60	52	5.02e-07	4.73e-15	61.21
	pymanopt-rcg	2.34e+02	1175	1175	1175	9.98e-06	5.68e-15	27.56
	pymanopt-rtr	2.34e+02	34	None	None	8.11e-08	5.68e-15	57.05
$p = 100$	cdopt-lbfgs	1.48e+02	561	579	579	8.89e-06	1.54e-12	6.28
	cdopt-cg	1.48e+02	1256	1875	1875	9.61e-06	3.99e-15	64.08
	cdopt-tr	1.48e+02	94	95	81	5.51e-08	4.16e-15	209.16
	pymanopt-rcg	1.48e+02	1535	1535	1535	9.45e-06	5.67e-15	57.02
	pymanopt-rtr	1.48e+02	44	None	None	6.09e-08	5.54e-15	405.36
$p = 200$	cdopt-lbfgs	1.30e+02	684	704	704	6.69e-06	5.37e-12	12.59
	cdopt-cg	1.30e+02	1157	1751	1751	8.68e-06	8.40e-14	74.15
	cdopt-tr	1.30e+02	64	65	57	5.77e-07	4.54e-15	224.90
	pymanopt-rcg	1.30e+02	1738	1738	1738	9.76e-06	4.73e-15	89.65
	pymanopt-rtr	1.30e+02	41	None	None	1.93e-07	4.75e-15	375.63

Table 8: Nearest correlation matrix problem on the ER dataset on GPUs.

		fval	iter	eval_f	eval_grad	stat	feas	time (s)
$p = 10$	cdopt-lbfgs	2.30e+03	182	192	192	9.95e-06	1.93e-14	0.47
	cdopt-cg	2.30e+03	230	346	346	8.40e-06	5.68e-15	0.72
	cdopt-tr	2.30e+03	75	76	71	2.74e-06	4.09e-15	2.23
	pymanopt-rcg	2.30e+03	314	314	314	9.56e-06	5.42e-15	0.74
	pymanopt-rtr	2.30e+03	41	None	None	2.75e-06	5.54e-15	1.42
$p = 20$	cdopt-cg	7.69e+02	256	374	374	9.39e-06	2.95e-14	1.36
	cdopt-lbfgs	7.69e+02	198	207	207	6.43e-06	4.49e-15	0.64
	cdopt-tr	7.69e+02	65	66	60	5.87e-06	4.12e-15	5.22
	pymanopt-rcg	7.69e+02	299	299	299	9.77e-06	5.74e-15	1.36
	pymanopt-rtr	7.69e+02	26	None	None	2.98e-08	5.74e-15	5.51
$p = 30$	cdopt-lbfgs	4.27e+02	318	328	328	9.92e-06	2.99e-15	1.31
	cdopt-cg	4.27e+02	731	1078	1078	6.17e-06	3.31e-14	4.27
	cdopt-tr	4.27e+02	78	79	71	2.05e-07	4.37e-15	6.30
	pymanopt-rcg	4.27e+02	711	711	711	8.85e-06	5.70e-15	5.16
	pymanopt-rtr	4.27e+02	31	None	None	1.59e-07	6.27e-15	8.06
$p = 50$	cdopt-lbfgs	2.34e+02	422	436	436	8.47e-06	1.60e-13	2.16
	cdopt-cg	2.34e+02	642	948	948	6.80e-06	5.35e-15	3.64
	cdopt-tr	2.34e+02	74	75	64	2.04e-06	4.50e-15	8.57
	pymanopt-rcg	2.34e+02	1194	1194	1194	7.26e-06	5.48e-15	7.24
	pymanopt-rtr	2.34e+02	34	None	None	4.58e-08	5.47e-15	23.41
$p = 100$	cdopt-lbfgs	1.48e+02	575	595	595	8.16e-06	1.45e-13	4.56
	cdopt-cg	1.48e+02	1045	1550	1550	9.90e-06	6.23e-14	8.59
	cdopt-tr	1.48e+02	91	92	81	5.27e-08	4.29e-15	25.19
	pymanopt-rcg	1.48e+02	2040	2040	2040	9.49e-06	5.76e-15	20.34
	pymanopt-rtr	1.48e+02	44	None	None	6.24e-08	5.56e-15	195.45
$p = 200$	cdopt-lbfgs	1.30e+02	671	701	701	9.55e-06	1.88e-11	10.67
	cdopt-cg	1.30e+02	1231	1856	1856	8.20e-06	3.47e-15	17.57
	cdopt-tr	1.30e+02	67	68	58	1.57e-07	4.40e-15	36.79
	pymanopt-rcg	1.30e+02	1794	1794	1794	9.13e-06	4.88e-15	34.44
	pymanopt-rtr	1.30e+02	41	None	None	1.46e-07	4.78e-15	186.64

7.3 Nonlinear eigenvalue problem

In this subsection, we test the numerical performance of the compared packages on solving the following smooth optimization problem over the Stiefel manifold:

$$\begin{aligned}
\min_{X \in \mathbb{R}^{n \times p}} \quad & f(X) = \frac{1}{2} \text{tr}(X^\top LX) + \frac{\alpha}{4} \rho(X)^\top L^\dagger \rho(X) \\
\text{s. t.} \quad & X^\top X = I_p,
\end{aligned} \tag{36}$$

Table 9: Nearest correlation matrix problem on the Lymph dataset on CPUs.

		fval	iter	eval_f	eval_grad	stat	feas	time (s)
$p = 10$	cdopt-lbfgs	1.93e+03	161	168	168	9.28e-06	2.62e-14	0.51
	cdopt-cg	1.93e+03	223	333	333	8.21e-06	4.25e-15	0.78
	cdopt-tr	1.93e+03	56	57	51	2.23e-06	4.19e-15	2.64
	pymanopt-rcg	1.93e+03	248	248	248	9.32e-06	5.25e-15	0.87
	pymanopt-rtr	1.93e+03	34	None	None	4.75e-10	5.37e-15	1.54
$p = 20$	cdopt-lbfgs	6.55e+02	217	226	226	9.55e-06	3.77e-15	0.89
	cdopt-cg	6.55e+02	349	524	524	9.28e-06	1.79e-14	6.41
	cdopt-tr	6.55e+02	60	61	58	2.23e-06	4.43e-15	20.18
	pymanopt-rcg	6.55e+02	462	462	462	9.22e-06	4.90e-15	11.64
	pymanopt-rtr	6.55e+02	31	None	None	2.07e-09	6.04e-15	17.35
$p = 30$	cdopt-lbfgs	3.56e+02	351	364	364	9.97e-06	3.78e-15	1.80
	cdopt-cg	3.56e+02	443	659	659	9.29e-06	3.98e-15	7.52
	cdopt-tr	3.56e+02	69	70	63	3.09e-07	4.06e-15	32.78
	pymanopt-rcg	3.56e+02	701	701	701	9.37e-06	5.43e-15	14.49
	pymanopt-rtr	3.56e+02	50	None	None	6.16e-07	5.58e-15	79.33
$p = 50$	cdopt-lbfgs	1.80e+02	374	389	389	9.64e-06	3.08e-15	2.40
	cdopt-cg	1.80e+02	738	1107	1107	6.52e-06	3.65e-15	29.03
	cdopt-tr	1.80e+02	60	61	55	9.36e-06	5.16e-15	40.50
	pymanopt-rcg	1.80e+02	993	993	993	9.97e-06	5.28e-15	25.93
	pymanopt-rtr	1.80e+02	46	None	None	3.40e-06	6.31e-15	42.89
$p = 100$	cdopt-lbfgs	1.03e+02	628	651	651	9.53e-06	1.51e-13	6.10
	cdopt-cg	1.03e+02	1437	2155	2155	9.95e-06	4.52e-15	69.45
	cdopt-tr	1.03e+02	89	90	76	1.79e-07	4.02e-15	170.99
	pymanopt-rcg	1.03e+02	2763	2763	2763	8.92e-06	5.33e-15	97.32
	pymanopt-rtr	1.03e+02	45	None	None	6.17e-07	5.18e-15	140.68
$p = 200$	cdopt-lbfgs	8.84e+01	522	540	540	8.97e-06	1.14e-11	8.44
	cdopt-cg	8.84e+01	716	1074	1074	9.94e-06	1.87e-13	42.01
	cdopt-tr	8.84e+01	58	59	49	2.71e-07	4.63e-15	155.79
	pymanopt-rcg	8.84e+01	2299	2299	2299	9.95e-06	4.35e-15	113.34
	pymanopt-rtr	8.84e+01	41	None	None	2.51e-08	4.53e-15	388.71

Table 10: Nearest correlation matrix problem on the Lymph dataset on GPUs.

		fval	iter	eval_f	eval_grad	stat	feas	time (s)
$p = 10$	cdopt-lbfgs	1.93e+03	156	162	162	9.65e-06	7.00e-15	0.39
	cdopt-cg	1.93e+03	208	320	320	9.59e-06	2.20e-14	0.56
	cdopt-tr	1.93e+03	55	56	50	6.21e-08	3.50e-15	1.74
	pymanopt-rcg	1.93e+03	248	248	248	9.36e-06	4.68e-15	0.48
	pymanopt-rtr	1.93e+03	34	None	None	3.73e-10	5.23e-15	1.11
$p = 20$	cdopt-lbfgs	6.55e+02	223	230	230	8.31e-06	3.85e-15	0.65
	cdopt-cg	6.55e+02	391	596	596	8.35e-06	2.97e-15	2.48
	cdopt-tr	6.55e+02	57	58	56	7.74e-06	4.04e-15	3.10
	pymanopt-rcg	6.55e+02	511	511	511	7.61e-06	5.01e-15	2.68
	pymanopt-rtr	6.55e+02	31	None	None	2.20e-09	5.99e-15	7.40
$p = 30$	cdopt-lbfgs	3.56e+02	357	373	373	8.49e-06	4.08e-15	1.20
	cdopt-cg	3.56e+02	463	699	699	6.43e-06	3.70e-15	2.29
	cdopt-tr	3.56e+02	69	70	63	3.21e-07	3.41e-15	4.99
	pymanopt-rcg	3.56e+02	614	614	614	8.79e-06	5.28e-15	5.38
	pymanopt-rtr	3.56e+02	50	None	None	6.18e-07	5.70e-15	31.51
$p = 50$	cdopt-lbfgs	1.80e+02	374	388	388	8.40e-06	3.58e-15	1.77
	cdopt-cg	1.80e+02	681	1005	1005	9.15e-06	2.38e-13	4.70
	cdopt-tr	1.80e+02	60	61	55	9.46e-06	5.62e-15	7.74
	pymanopt-rcg	1.80e+02	1130	1130	1130	7.61e-06	5.20e-15	8.27
	pymanopt-rtr	1.80e+02	46	None	None	3.08e-06	6.03e-15	17.18
$p = 100$	cdopt-lbfgs	1.03e+02	641	657	657	7.87e-06	2.76e-14	4.75
	cdopt-cg	1.03e+02	1615	2417	2417	9.72e-06	4.83e-15	12.77
	cdopt-tr	1.03e+02	88	89	75	4.76e-06	4.52e-15	22.09
	pymanopt-rcg	1.03e+02	2734	2734	2734	9.20e-06	5.33e-15	28.66
	pymanopt-rtr	1.03e+02	45	None	None	1.01e-06	5.26e-15	66.00
$p = 200$	cdopt-lbfgs	8.84e+01	519	537	537	9.32e-06	3.92e-12	7.19
	cdopt-cg	8.84e+01	611	923	923	8.56e-06	9.29e-15	7.33
	cdopt-tr	8.84e+01	56	57	49	5.78e-06	8.23e-15	26.17
	pymanopt-rcg	8.84e+01	1937	1937	1937	9.03e-06	4.34e-15	33.71
	pymanopt-rtr	8.84e+01	41	None	None	2.52e-08	4.38e-15	201.75

where $\rho(X) := \text{diag}(XX^\top)$, L is a tridiagonal matrix with 2 as its diagonal entries and -1 as its subdiagonal and superdiagonal entries. Moreover, L^\dagger refers to the pseudo-inverse of L . Problem (36), arisen from electronic structure calculation, has become a standard testing problem for investigating the convergence of self-consistent field methods due to its simplicity [42].

In all the numerical experiments of this subsection, we provide the expression of the function value, the gradient, and the Hessian-vector product, and set the numerical backends for CDOpt and PyManopt as Numpy. We choose

the L-BFGS, CG, and trust-region solvers from SciPy to test the numerical performance of CDOpt. For comparison, we choose the Riemannian CG solver and Riemannian trust-region solver from PyManopt since L-BFGS is not available in PyManopt. All the hyperparameters of these solvers are fixed by the same settings in Section 7.2. Furthermore, following the techniques in [63], we first randomly generate a reference point $\tilde{X} \in \mathcal{S}_{n,p}$, and generate the initial point X_{init} as the eigenvectors that corresponds to the largest p eigenvalues of $L + \alpha \cdot \text{Diag}(L^\dagger \rho(\tilde{X}))$.

Table 11 and Table 12 present the numerical results on the comparison of CDOpt and PyManopt, and the detailed meanings of their column headers are given in Table 6. From Table 11 and Table 12, we can observe that CDOpt achieves the same function values in comparable iterations as PyManopt in all the tested instances. Moreover, CDOpt shows comparable performance in the aspect of CPU time for large-scale problems, especially when p is large.

Table 11: Test results on nonlinear eigenvalue problems with $n = 1000$.

		fval	iter	eval_f	eval_grad	stat	feas	time (s)
$p = 10$	cdopt-lbfgs	3.57e+01	106	116	116	8.42e-06	6.52e-14	0.20
	cdopt-cg	3.57e+01	100	181	181	7.43e-06	1.11e-13	0.14
	cdopt-tr	3.57e+01	20	21	19	8.23e-06	4.26e-15	0.13
	pymanopt-rcg	3.57e+01	62	62	62	6.74e-06	1.40e-15	0.15
	pymanopt-rtr	3.57e+01	13	None	None	2.84e-06	1.62e-15	0.55
$p = 20$	cdopt-lbfgs	2.11e+02	166	175	175	8.10e-06	1.33e-14	1.60
	cdopt-cg	2.11e+02	168	268	268	5.72e-06	5.62e-14	1.35
	cdopt-tr	2.11e+02	31	32	28	2.58e-07	1.18e-15	2.71
	pymanopt-rcg	2.11e+02	160	160	160	9.40e-06	1.94e-15	1.16
	pymanopt-rtr	2.11e+02	11	None	None	8.31e-07	1.30e-15	1.50
$p = 30$	cdopt-lbfgs	6.48e+02	301	324	324	7.61e-06	1.77e-15	7.82
	cdopt-cg	6.48e+02	325	528	528	8.28e-06	5.76e-15	4.36
	cdopt-tr	6.48e+02	32	33	30	4.01e-07	1.67e-15	3.04
	pymanopt-rcg	6.48e+02	458	458	458	2.39e-05	2.45e-15	5.88
	pymanopt-rtr	6.48e+02	9	None	None	1.60e-07	1.84e-15	2.55
$p = 50$	cdopt-lbfgs	2.81e+03	407	425	425	8.02e-06	3.10e-14	16.34
	cdopt-cg	2.81e+03	431	682	682	4.75e-06	1.43e-15	7.41
	cdopt-tr	2.81e+03	37	38	35	9.33e-07	1.91e-15	6.54
	pymanopt-rcg	2.81e+03	423	423	423	4.13e-05	2.27e-15	8.40
	pymanopt-rtr	2.81e+03	10	None	None	3.07e-10	3.87e-15	8.56
$p = 100$	cdopt-lbfgs	2.16e+04	732	773	773	2.70e-05	8.30e-15	38.17
	cdopt-cg	2.16e+04	999	1632	1620	4.86e-05	2.75e-15	25.77
	cdopt-tr	2.16e+04	58	59	56	6.50e-07	2.41e-15	22.04
	pymanopt-rcg	2.16e+04	854	854	854	5.28e-04	3.80e-15	25.24
	pymanopt-rtr	2.16e+04	12	None	None	1.55e-08	5.52e-15	23.49

7.4 Training orthogonally constrained neural network

In this subsection, we test the numerical performance of CDOpt on training orthogonally constrained deep neural networks (DNNs). Moreover, we compare the numerical performance of CDOpt with existing Riemannian optimization packages GeoTorch and McTorch. It is worth mentioning that although GeoOpt is designed for training neural networks, it is not easy to be used in practice. When applied to training neural networks, GeoOpt requires the users to write the layers themselves from PyTorch.nn modules, including designing the `__init__()` function that specifies the constrained manifold, the `forward()` function that involves geometrical materials, and the `reset_parameters()`

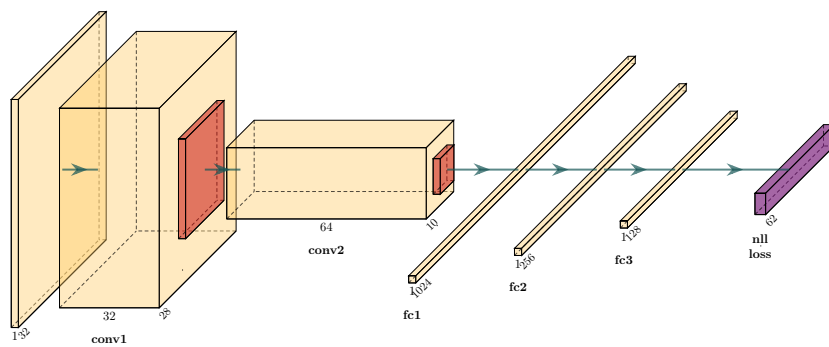
Table 12: Test results on nonlinear eigenvalue problems with $n = 3000$.

		fval	iter	eval_f	eval_grad	stat	fcons	time (s)
$p = 10$	cdopt-lbfgs	3.57e+01	128	140	140	7.54e-06	1.42e-14	2.04
	cdopt-cg	3.57e+01	114	201	201	8.14e-06	1.60e-13	0.97
	cdopt-tr	3.57e+01	24	25	23	2.84e-08	5.32e-16	1.58
	pymanopt-rcg	3.57e+01	81	81	81	9.25e-06	8.93e-16	0.89
	pymanopt-rtr	3.57e+01	8	None	None	8.39e-09	1.01e-15	5.69
$p = 20$	cdopt-lbfgs	2.11e+02	148	159	159	6.52e-06	7.46e-13	6.39
	cdopt-cg	2.11e+02	145	209	209	9.22e-06	5.58e-13	2.81
	cdopt-tr	2.11e+02	19	20	18	3.26e-06	3.15e-15	2.04
	pymanopt-rcg	2.11e+02	136	136	136	9.69e-06	1.94e-15	2.19
	pymanopt-rtr	2.11e+02	11	None	None	7.14e-07	1.46e-15	12.63
$p = 30$	cdopt-lbfgs	6.48e+02	239	255	255	9.56e-06	1.45e-14	11.04
	cdopt-cg	6.48e+02	284	456	456	8.09e-06	8.29e-15	4.81
	cdopt-tr	6.48e+02	32	33	29	4.42e-08	1.53e-15	6.03
	pymanopt-rcg	6.48e+02	374	374	374	2.42e-05	1.82e-15	7.10
	pymanopt-rtr	6.48e+02	9	None	None	3.78e-08	2.46e-15	19.06
$p = 50$	cdopt-lbfgs	2.81e+03	396	418	418	9.48e-06	7.22e-15	35.26
	cdopt-cg	2.81e+03	293	462	462	9.54e-06	5.77e-15	8.45
	cdopt-tr	2.81e+03	46	47	41	5.19e-07	1.70e-15	13.47
	pymanopt-rcg	2.81e+03	328	328	328	2.90e-05	2.81e-15	9.19
	pymanopt-rtr	2.81e+03	9	None	None	5.94e-06	4.28e-15	23.60
$p = 100$	cdopt-lbfgs	2.16e+04	704	738	738	9.84e-05	2.17e-14	98.69
	cdopt-cg	2.16e+04	645	1014	1014	5.86e-05	7.02e-14	38.70
	cdopt-tr	2.16e+04	48	49	47	9.30e-08	2.16e-15	71.15
	pymanopt-rcg	2.16e+04	580	580	580	2.33e-04	3.82e-15	38.05
	pymanopt-rtr	2.16e+04	9	None	None	1.63e-08	5.73e-15	75.66

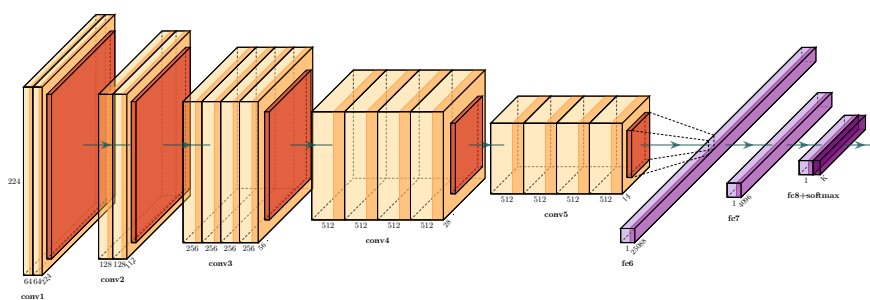
function that reset the parameters to generate a feasible point for training. Therefore, we compare CDOpt only with GeoTorch and McTorch.

Our first test example is to train a modified LeNet [39] for classification on the EMNIST-bymerge dataset [14], which is a set of handwritten character digits derived from the NIST Special Database 19 and converted to a 28×28 pixel image format and dataset structure that directly matches the MNIST dataset. The EMNIST-bymerge dataset has 697932 training samples and 116323 test samples in 47 classes. As illustrated in Figure 3(a), the network has 3 convolution layers and 3 fully-connected layers, and we impose the orthogonal constraints on the weight matrix of the first fully-connected layer. Moreover, we also choose to train VGG19 [53] for classification on the CIFAR-10 dataset [38]. CIFAR-10 dataset has 50000 training samples and 10000 test samples that are divided into 10 classes. The VGG19 network contains 16 convolution layers and 3 fully-connected layers as illustrated in Figure 3(b). Furthermore, we train Densenet121 [32] for classification on the CIFAR-100 dataset [38], which has 100 classes in total, with 500 training images and 100 testing images in each class. Similar to LeNet, we impose the orthogonal constraints on the weight matrix of the first fully-connected layer of VGG19 and Densenet.

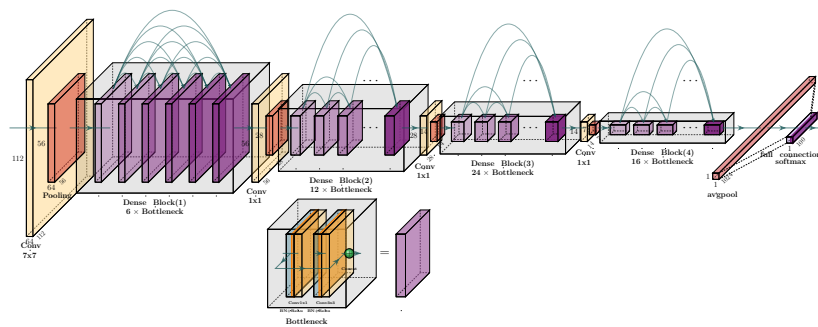
In training these orthogonally constrained neural networks by CDOpt, we choose the PyTorch build-in unconstrained optimizers SGD and Adam, together with the AdaMod, Lookahead, and Ranger from the PyTorch-optimizer packages. Developed from the trivialization approaches, GeoTorch is also compatible to existing unconstrained optimizers, hence we try to apply SGD, Adam, AdaMod, Lookahead, and Ranger to train these orthogonally constrained networks through GeoTorch. However, among all the aforementioned solvers, only Riemannian SGD is provided in McTorch package. Therefore, we only use the Riemannian SGD from the McTorch package to train these networks.



(a) LeNet



(b) VGG19



(c) Densnet121

Fig. 3: The structure of the tested neural networks.

In training the modified LeNet, the batchsize is set as 64, the total number of epochs is set as 30, and the learning rate is set as 0.02 for SGD with momentum parameter as 0.9, 0.001 for Adam [36] and AdaMod [15], 0.3 for Ranger [62] and 0.01 for the base optimizer Yogi [67] in Lookahead [70] optimizer. For training VGG19 and Densenet121, the batchsize is fixed as 256, the total number of epochs is set as 300, while the learning rate is set as 0.01 for SGD (with momentum parameter as 0.9), 3×10^{-4} for Adam, AdaMod, and Diff-Grad, and 0.3 for Ranger and 0.01 for the base optimizer Yogi in Lookahead optimizer. Moreover, we choose the learning rate decrease strategy for all these optimizers and decrease the learning rate by multiplying a factor after every epoch. Such factor is set as 0.9 in training LeNet, and 0.99 in training VGG. Furthermore, when applying CDOpt in training these networks, the penalty parameter β in the constraint dissolving approaches is fixed as 0.01 for all the test instances.

Table 13 exhibits the results of the numerical experiments, where the detailed meanings of the column headers are given in Table 6. Compared with GeoTorch, CDOpt achieves similar accuracy and is compatible with various of unconstrained optimizers from PyTorch and PyTorch-optimizer. However, as computing the matrix exponential function and matrix inverse are expensive on GPU, GeoTorch takes significantly longer CPU time and costs more memory than CDOpt.

Furthermore, CDOpt achieves similar accuracy as McTorch. However, training manifold constrained neural networks by CDOpt only requires matrix-matrix multiplication, while the optimizers in McTorch involve computing the retractions in each iteration by singular value decomposition. Therefore, running unconstrained SGD by CDOpt is slightly faster than running the Riemannian SGD by McTorch. Moreover, in the presence of difficulties in developing efficient Riemannian solvers, existing PyTorch-based Riemannian solvers are limited. For example, McTorch only provides Riemannian SGD and Riemannian AdaGrad. In contrast, training manifold constrained neural networks by CDOpt is highly adaptive to various existing unconstrained solvers.

Table 13: Numerical results on orthogonally constrained deep neural networks.

		LeNet + EMNIST-byclass			VGG 19 + CIFAR-10			Densenet121 + CIFAR-100		
		acc	feas	time/epoch	acc	feas	time/epoch	acc	feas	time/epoch
SGD	CDOpt	91.07	2.91e-03	68.77	92.81	4.56e-03	54.14	76.74	3.21e-03	50.29
	GeoTorch	91.04	4.25e-03	292.55		out of memory		76.70	4.87e-03	56.20
	McTorch	91.05	3.52e-03	89.41	92.70	5.15e-03	74.75	76.45	3.39e-03	52.76
Adam	CDOpt	91.02	5.39e-03	69.71	92.70	7.75e-03	57.89	72.13	2.37e-03	52.57
	GeoTorch	91.05	4.22e-03	294.83		out of memory		71.35	4.61e-03	54.96
	McTorch		not implemented			not implemented			not implemented	
AdaMod	CDOpt	91.06	3.81e-03	82.53	92.58	4.38e-03	58.78	73.96	2.95e-03	56.10
	GeoTorch	91.05	4.32e-03	319.62		out of memory		73.67	4.83e-03	58.14
	McTorch		not implemented			not implemented			not implemented	
Ranger	CDOpt	91.11	3.37e-03	76.16	92.76	6.29e-03	57.93	73.28	2.35e-03	52.71
	GeoTorch	90.96	4.25e-03	298.07		out of memory		73.39	4.49e-03	57.91
	McTorch		not implemented			not implemented			not implemented	
Lookahead	CDOpt	91.07	3.71e-03	83.15	92.97	4.69e-03	59.66	74.38	3.31e-03	54.22
	GeoTorch	91.01	4.25e-03	295.93		out of memory		74.50	4.53e-03	60.58
	McTorch		not implemented			not implemented			not implemented	

8 Conclusion

In this paper, we consider how to practically implement constraint dissolving approaches to solve Riemannian optimization problem OCP. We first analyze the relationships between OCP and CDF under RCRCQ conditions, which is weaker than the assumptions in [64]. Moreover, we propose a novel scheme for determining the threshold value of the penalty parameter β in CDF, which only involves the evaluations of f , \mathcal{A} , c , and their derivatives. We prove that with any penalty parameter β greater than the suggested threshold value, CDF and OCP have the same first-order stationary points, second-order stationary points, and local minimums in a neighborhood of \mathcal{M} . In addition, based on the Monte Carlo sampling technique, we provide a practical scheme for choosing the penalty parameter β in CDF.

Furthermore, we introduce the Python library package CDOpt for manifold optimization. CDOpt serves as a complementary package to existing Riemannian optimization packages, in the sense that it enables direct implementations of various existing unconstrained optimization solvers for Riemannian optimization through the constraint dissolving approaches. CDOpt has user-friendly interfaces and supports various important features from its supported numerical backends, such as GPU/TPU supports, automatic differentiation, distributed training, JIT compilation, etc. Moreover, CDOpt only requires the expression of $c(x)$ in defining a new manifold. Therefore, users can enjoy great convenience in defining and solving a wide range of manifold constrained optimization problems, without any knowledge of the geometrical materials in differential geometry. Furthermore, CDOpt provides various predefined neural layers for PyTorch and Flax, which enables the users to build and train the manifold constrained neural networks only with minor modification to the standard PyTorch/JAX codes. Preliminary numerical experiments further demonstrate the high efficiency of CDOpt, which can achieve comparable or superior performance when compared with existing state-of-the-art Riemannian optimization packages.

CDOpt is still under active development, and some of the future works include adding supports for other numerical backends (e.g., TensorFlow, MindSpore, PaddlePaddle), and integrate CDOpt with more optimization frameworks, such as horovod and Apex for distributed training, FATE for federated learning, and BoTorch for Bayesian optimization.

References

1. Abadi, M., Agarwal, A., Barham, P., Brevdo, E., Chen, Z., Citro, C., Corrado, G.S., Davis, A., Dean, J., Devin, M., Ghemawat, S., Goodfellow, I., Harp, A., Irving, G., Isard, M., Jia, Y., Jozefowicz, R., Kaiser, L., Kudlur, M., Levenberg, J., Mané, D., Monga, R., Moore, S., Murray, D., Olah, C., Schuster, M., Shlens, J., Steiner, B., Sutskever, I., Talwar, K., Tucker, P., Vanhoucke, V., Vasudevan, V., Viégas, F., Vinyals, O., Warden,

- P., Wattenberg, M., Wicke, M., Yu, Y., Zheng, X.: TensorFlow: Large-scale machine learning on heterogeneous systems (2015). URL <https://www.tensorflow.org/>. Software available from tensorflow.org
2. Ablin, P., Peyré, G.: Fast and accurate optimization on the orthogonal manifold without retraction. In: International Conference on Artificial Intelligence and Statistics, pp. 5636–5657. PMLR (2022)
 3. Ablin, P., Vary, S., Gao, B., Absil, P.A.: Infeasible deterministic, stochastic, and variance-reduction algorithms for optimization under orthogonality constraints. arXiv preprint arXiv:2303.16510 (2023)
 4. Absil, P.A., Mahony, R., Sepulchre, R.: Optimization algorithms on matrix manifolds. Princeton University Press (2009)
 5. Arjovsky, M., Shah, A., Bengio, Y.: Unitary evolution recurrent neural networks. In: International Conference on Machine Learning, pp. 1120–1128. PMLR (2016)
 6. Bai, Z., Li, R.C.: Minimization principles for the linear response eigenvalue problem i: Theory. *SIAM Journal on Matrix Analysis and Applications* **33**(4), 1075–1100 (2012)
 7. Bai, Z., Li, R.C.: Minimization principles and computation for the generalized linear response eigenvalue problem. *BIT Numerical Mathematics* **54**(1), 31–54 (2014)
 8. Bansal, N., Chen, X., Wang, Z.: Can we gain more from orthogonality regularizations in training deep networks? In: Advances in Neural Information Processing Systems, vol. 31 (2018)
 9. Bendokat, T., Zimmermann, R., Absil, P.A.: A Grassmann manifold handbook: Basic geometry and computational aspects. *Advances in Computational Mathematics* **50**(1), 6 (2024)
 10. Blondel, M., Berthet, Q., Cuturi, M., Frostig, R., Hoyer, S., Llinares-Lopez, F., Pedregosa, F., Vert, J.P.: Efficient and modular implicit differentiation. In: Advances in Neural Information Processing Systems, vol. 35, pp. 5230–5242 (2022)
 11. Boumal, N.: An introduction to optimization on smooth manifolds. Cambridge University Press (2023)
 12. Boumal, N., Mishra, B., Absil, P.A., Sepulchre, R.: Manopt, a Matlab toolbox for optimization on manifolds. *Journal of Machine Learning Research* **15**(1), 1455–1459 (2014)
 13. Bradbury, J., Frostig, R., Hawkins, P., Johnson, M.J., Leary, C., Maclaurin, D., Necula, G., Paszke, A., VanderPlas, J., Wanderman-Milne, S., Zhang, Q.: JAX: Composable transformations of Python+NumPy programs (2018). URL <http://github.com/google/jax>
 14. Cohen, G., Afshar, S., Tapson, J., Van Schaik, A.: EMNIST: Extending MNIST to handwritten letters. In: 2017 international joint conference on neural networks (IJCNN), pp. 2921–2926. IEEE (2017)
 15. Ding, J., Ren, X., Luo, R., Sun, X.: An adaptive and momental bound method for stochastic learning. arXiv preprint arXiv:1910.12249 (2019)
 16. Edelman, A., Arias, T.A., Smith, S.T.: The geometry of algorithms with orthogonality constraints. *SIAM Journal on Matrix Analysis and Appli-*

- cations **20**(2), 303–353 (1998)
17. Estrin, R., Friedlander, M.P., Orban, D., Saunders, M.A.: Implementing a smooth exact penalty function for equality-constrained nonlinear optimization. *SIAM Journal on Scientific Computing* **42**(3), A1809–A1835 (2020)
 18. Feinman, R.: PyTorch-minimize: Newton and Quasi-Newton optimization with PyTorch (2022). URL <https://github.com/rfeinman/pytorch-minimize>
 19. Fletcher, R., Leyffer, S.: Nonlinear programming without a penalty function. *Mathematical Programming* **91**(2), 239–269 (2002)
 20. Fletcher, R., Reeves, C.M.: Function minimization by conjugate gradients. *The Computer Journal* **7**(2), 149–154 (1964)
 21. Gao, B., Son, N.T., Absil, P.A., Stykel, T.: Riemannian optimization on the symplectic Stiefel manifold. *SIAM Journal on Optimization* **31**(2), 1546–1575 (2021)
 22. Gao, B., Vary, S., Ablin, P., Absil, P.A.: Optimization flows landing on the stiefel manifold. *IFAC-PapersOnLine* **55**(30), 25–30 (2022)
 23. Glorot, X., Bengio, Y.: Understanding the difficulty of training deep feed-forward neural networks. In: *Proceedings of the Thirteenth International Conference on Artificial Intelligence and Statistics, Proceedings of Machine Learning Research*, vol. 9, pp. 249–256. PMLR, Chia Laguna Resort, Sardinia, Italy (2010)
 24. Golub, G.H., Van Loan, C.F.: *Matrix computations*. JHU press (2013)
 25. Goyens, F., Eftekhari, A., Boumal, N.: Computing second-order points under equality constraints: revisiting Fletcher’s augmented Lagrangian. *Journal of Optimization Theory and Applications* pp. 1–31 (2024)
 26. Harris, C.R., Millman, K.J., van der Walt, S.J., Gommers, R., Virtanen, P., Cournapeau, D., Wieser, E., Taylor, J., Berg, S., Smith, N.J., et al.: Array programming with NumPy. *Nature* **585**(7825), 357–362 (2020)
 27. Heek, J., Levskaya, A., Oliver, A., Ritter, M., Rondepierre, B., Steiner, A., van Zee, M.: Flax: A neural network library and ecosystem for JAX (2020). URL <http://github.com/google/flax>
 28. Hu, J., Liu, X., Wen, Z.W., Yuan, Y.X.: A brief introduction to manifold optimization. *Journal of the Operations Research Society of China* **8**(2), 199–248 (2020)
 29. Hu, X., Liu, X.: An efficient orthonormalization-free approach for sparse dictionary learning and dual principal component pursuit. *Sensors* **20**(3041) (2020)
 30. Hu, X., Xiao, N., Liu, X., Toh, K.C.: A constraint dissolving approach for nonsmooth optimization over the stiefel manifold. *IMA Journal of Numerical Analysis* p. drad098 (2023)
 31. Hu, X., Xiao, N., Liu, X., Toh, K.C.: An improved unconstrained approach for bilevel optimization. *SIAM Journal on Optimization* **33**(4), 2801–2829 (2023)
 32. Huang, G., Liu, Z., Van Der Maaten, L., Weinberger, K.Q.: Densely connected convolutional networks. In: *Proceedings of the IEEE Conference*

- on Computer Vision and Pattern Recognition, pp. 4700–4708 (2017)
33. Huang, L., Liu, X., Lang, B., Yu, A.W., Wang, Y., Li, B.: Orthogonal weight normalization: Solution to optimization over multiple dependent Stiefel manifolds in deep neural networks. In: Thirty-Second AAAI Conference on Artificial Intelligence (2018)
 34. Huang, W., Absil, P.A., Gallivan, K.A., Hand, P.: ROPTLIB: an object-oriented C++ library for optimization on Riemannian manifolds. *ACM Transactions on Mathematical Software* **44**(4), 1–21 (2018)
 35. Huang, W., Wei, M., Gallivan, K.A., Van Dooren, P.: A Riemannian optimization approach to clustering problems. *arXiv preprint arXiv:2208.03858* (2022)
 36. Kingma, D.P., Ba, J.: Adam: A method for stochastic optimization. *arXiv preprint arXiv:1412.6980* (2014)
 37. Kochurov, M., Karimov, R., Kozlukov, S.: Geoopt: Riemannian optimization in PyTorch. *arXiv preprint arXiv:2005.02819* (2020)
 38. Krizhevsky, A., Hinton, G., et al.: Learning multiple layers of features from tiny images (2009)
 39. LeCun, Y., Boser, B., Denker, J.S., Henderson, D., Howard, R.E., Hubbard, W., Jackel, L.D.: Backpropagation applied to handwritten zip code recognition. *Neural Computation* **1**(4), 541–551 (1989)
 40. Lezcano Casado, M.: Trivializations for gradient-based optimization on manifolds. In: *Advances in Neural Information Processing Systems*, vol. 32 (2019)
 41. Li, L., Toh, K.C.: An inexact interior point method for l_1 -regularized sparse covariance selection. *Mathematical Programming Computation* **2**(3), 291–315 (2010)
 42. Lin, L., Yang, C.: Elliptic preconditioner for accelerating the self-consistent field iteration in kohn–sham density functional theory. *SIAM Journal on Scientific Computing* **35**(5), S277–S298 (2013)
 43. Maclaurin, D., Duvenaud, D., Johnson, M., Adams, R.P.: Autograd: Reverse-mode differentiation of native Python. In: *ICML workshop on Automatic Machine Learning* (2015)
 44. Marion, J., Mathews, J., Schmidler, S.C.: Finite-sample complexity of sequential Monte Carlo estimators. *The Annals of Statistics* **51**(3), 1357 – 1375 (2023)
 45. Meghwanshi, M., Jawanpuria, P., Kunchukuttan, A., Kasai, H., Mishra, B.: McTorch, a manifold optimization library for deep learning. Tech. rep., *arXiv preprint arXiv:1810.01811* (2018)
 46. Minchenko, L., Stakhovskii, S.: On relaxed constant rank regularity condition in mathematical programming. *Optimization* **60**(4), 429–440 (2011)
 47. Miolane, N., Guigui, N., Brigant, A.L., Mathe, J., Hou, B., Thanwerdas, Y., Heyder, S., Peltre, O., Koep, N., Zaatiti, H., Hajri, H., Cabanes, Y., Gerald, T., Chauchat, P., Shewmake, C., Brooks, D., Kainz, B., Donnat, C., Holmes, S., Penneec, X.: Geomstats: A python package for Riemannian geometry in machine learning. *Journal of Machine Learning Research* **21**(223), 1–9 (2020)

48. Nickel, M., Kiela, D.: Learning continuous hierarchies in the Lorentz model of hyperbolic geometry. In: International Conference on Machine Learning, pp. 3779–3788. PMLR (2018)
49. Nocedal, J., Wright, S.: Numerical optimization. Springer Science & Business Media (2006)
50. Paszke, A., Gross, S., Massa, F., Lerer, A., Bradbury, J., Chanan, G., Killeen, T., Lin, Z., Gimelshein, N., Antiga, L., Desmaison, A., Kopf, A., Yang, E., DeVito, Z., Raison, M., Tejani, A., Chilamkurthy, S., Steiner, B., Fang, L., Bai, J., Chintala, S.: PyTorch: An imperative style, high-performance deep learning library. In: Advances in Neural Information Processing Systems, vol. 32 (2019)
51. Powell, M., Yuan, Y.: A trust region algorithm for equality constrained optimization. *Mathematical Programming* **49**(1), 189–211 (1991)
52. Ragonneau, T.M., Zhang, Z.: PDFO: a cross-platform package for Powell’s derivative-free optimization solvers (2023)
53. Simonyan, K., Zisserman, A.: Very deep convolutional networks for large-scale image recognition. *arXiv preprint arXiv:1409.1556* (2014)
54. Son, N.T., Absil, P.A., Gao, B., Stykel, T.: Computing symplectic eigenpairs of symmetric positive-definite matrices via trace minimization and Riemannian optimization. *SIAM Journal on Matrix Analysis and Applications* **42**(4), 1732–1757 (2021)
55. Steihaug, T.: The conjugate gradient method and trust regions in large scale optimization. *SIAM Journal on Numerical Analysis* **20**(3), 626–637 (1983)
56. Toint, P.: Towards an efficient sparsity exploiting Newton method for minimization. In: *Sparse matrices and their uses*, pp. 57–88. Academic Press (1981)
57. Townsend, J., Koep, N., Weichwald, S.: Pymanopt: A python toolbox for optimization on manifolds using automatic differentiation. *Journal of Machine Learning Research* **17**(137), 1–5 (2016)
58. Tsakiris, M.C., Vidal, R.: Dual principal component pursuit. *Journal of Machine Learning Research* **19**(18), 1–50 (2018)
59. Utpala, S., Han, A., Jawanpuria, P., Mishra, B.: Rieoptax: Riemannian optimization in JAX. *arXiv preprint arXiv:2210.04840* (2022)
60. Virtanen, P., Gommers, R., Oliphant, T.E., Haberland, M., Reddy, T., Cournapeau, D., Burovski, E., Peterson, P., Weckesser, W., Bright, J., et al.: Scipy 1.0: fundamental algorithms for scientific computing in python. *Nature methods* **17**(3), 261–272 (2020)
61. Wang, J., Chen, Y., Chakraborty, R., Yu, S.X.: Orthogonal convolutional neural networks. In: *Proceedings of the IEEE/CVF Conference on Computer Vision and Pattern Recognition*, pp. 11505–11515 (2020)
62. Wright, L.: New deep learning optimizer, Ranger: Synergistic combination of RAdam + Lookahead for the best of both. Github <https://github.com/lessw2020/Ranger-Deep-Learning-Optimizer> **8** (2019)
63. Xiao, N., Liu, X.: Solving optimization problems over the Stiefel manifold by smooth exact penalty function. *arXiv preprint arXiv:2110.08986* (2021)

64. Xiao, N., Liu, X., Toh, K.C.: Dissolving constraints for Riemannian optimization. *Mathematics of Operations Research* **49**(1), 366–397 (2024)
65. Xiao, N., Liu, X., Yuan, Y.x.: A class of smooth exact penalty function methods for optimization problems with orthogonality constraints. *Optimization Methods and Software* pp. 1–37 (2020)
66. Xiao, N., Liu, X., Yuan, Y.x.: Exact penalty function for $\ell_{2,1}$ norm minimization over the Stiefel manifold. *SIAM Journal on Optimization* **31**(4), 3097–3126 (2021)
67. Zaheer, M., Reddi, S., Sachan, D., Kale, S., Kumar, S.: Adaptive methods for nonconvex optimization. In: *Advances in Neural Information Processing Systems*, vol. 31 (2018)
68. Zavala, V.M., Anitescu, M.: Scalable nonlinear programming via exact differentiable penalty functions and trust-region Newton methods. *SIAM Journal on Optimization* **24**(1), 528–558 (2014)
69. Zhai, Y., Yang, Z., Liao, Z., Wright, J., Ma, Y.: Complete dictionary learning via L4-norm maximization over the orthogonal group. *Journal of Machine Learning Research* **21**(165), 1–68 (2020)
70. Zhang, M., Lucas, J., Ba, J., Hinton, G.E.: Lookahead optimizer: k steps forward, 1 step back. In: *Advances in Neural Information Processing Systems*, vol. 32 (2019)
71. Zhou, J., Do, M.N., Kovacevic, J.: Special paraunitary matrices, Cayley transform, and multidimensional orthogonal filter banks. *IEEE Transactions on Image Processing* **15**(2), 511–519 (2006)

Acknowledgements The numerical experiments in this paper are performed on the supercomputing system in the Supercomputing Center of Hangzhou City University.

The authors thank Professor Pierre-Antoine Absil for his helpful comments and discussions on Riemannian optimization approaches. The authors also thank the editors and anonymous reviewers for their valuable suggestions to improve the paper.

Ethics Declarations

Funding

The research of Kim-Chuan Toh and Nachuan Xiao is supported by the Ministry of Education, Singapore, under its Academic Research Fund Tier 3 grant call (MOE-2019-T3-1-010). The research of Xiaoyin Hu is supported by the National Natural Science Foundation of China (Grant No. 12301408), Zhejiang Provincial Natural Science Foundation of China under Grant (No. LQ23A010002). The research of Xin Liu is supported in part by the National Natural Science Foundation of China (No. 12125108, 11971466, 12288201, 12021001, 11991021) and Key Research Program of Frontier Sciences, Chinese Academy of Sciences (No. ZDBS-LY-7022).

Conflict of interest

The authors declare that they have no conflict of interest.

Availability of data and materials

All data analyzed during this study are publicly available. URLs are included in this published article.

Code availability

The full code was made available for review. We remark that a set of packages were used in this study, that were either open source or available for academic use. Specific references are included in this published article.